Transport at high beta in the NSTX spherical tokamak

Walter Guttenfelder[1], R.E. Bell[1], E. Belova[1], J. Candy[2], J.M. Canik[3],N. Crocker[4], E. Fredrickson[1], S.P. Gerhardt[1], N. Gorelenkov[1], S.M. Kaye[1], B.P. LeBlanc[1], R. Maingi[1], J. Menard[1], D. Mueller[1], R. Raman[5], Y. Ren[1], J. Ruiz-Ruiz[6], F. Scotti[7], D.R. Smith[8], K. Tritz[9], W.X. Wang[1], H. Yuh[10]

[1]PPPL, [2]General Atomics, [3]ORNL, [4]UCLA, [5]U-Washington, [6]MIT, [7]LLNL, [8]UW-Madison, [9]Johns-Hopkins, [10]Nova Photonics, Inc.

US-Japan Compact Toroid Workshop
Irvine, CA, Aug. 22-24, 2016

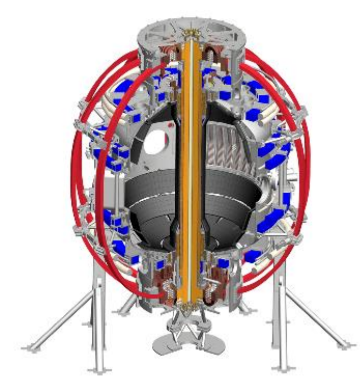

Outline

- Spherical tokamak configuration and general NSTX transport observations ($\chi_i \sim \chi_{i,NC}$, $\tau_E \sim 1/\nu$)

- Discussion of theoretical transport mechanisms, validation efforts and plans
  - Drift waves in core
  - Drift waves in H-mode edge pedestal
  - Electron transport by fast-ion-driven Alfven eigenmodes

- NSTX-Upgrade & first operation

Spherical tokamak (ST) has aspect ratio A<2, many parameters intermediate to tokamak, FRC

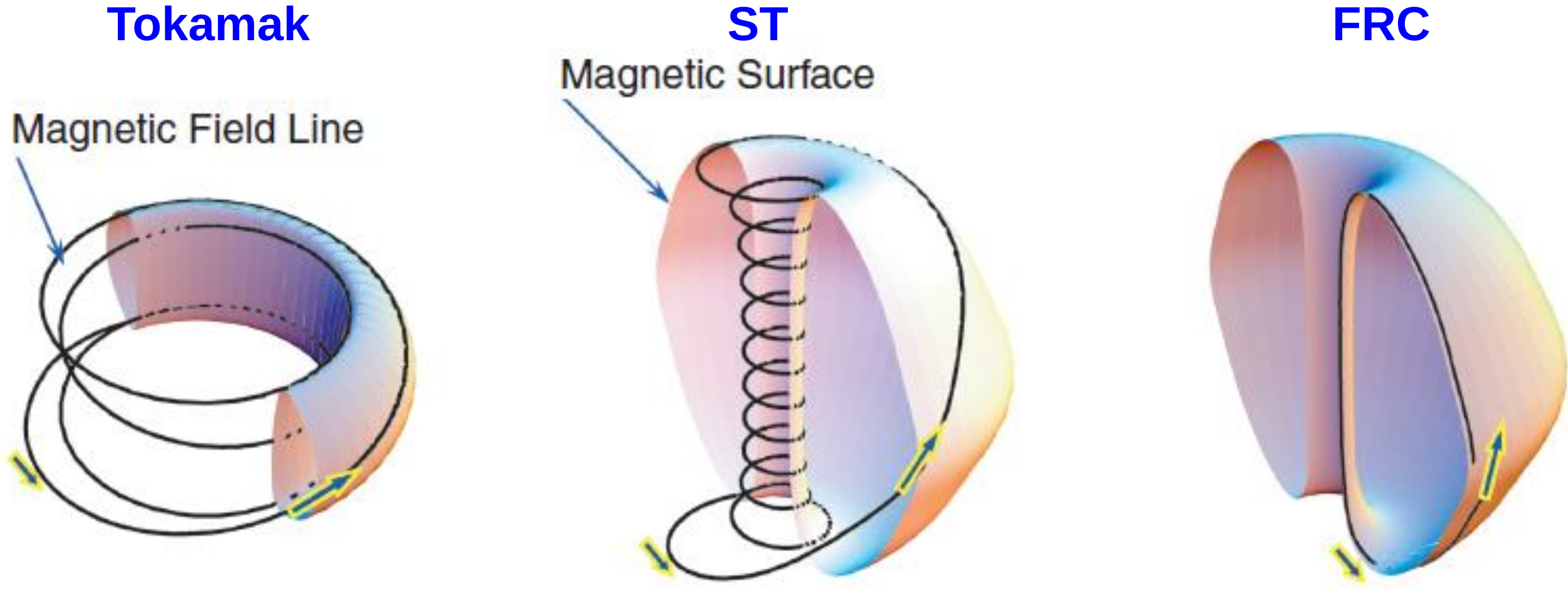

	Tokamak	ST	FRC
A=R/a	3	1.2-2	1
q	3-4	6-20	~0
β	3-10%	10-40%	100%
$\rho_*=\rho_i/a$	1/200	1/100	1/30

- ST is naturally elongated, favorable average curvature improves MHD stability, allowing higher β & use of smaller B_T

Toroidicity drives interchange-like electrostatic ballooning mode instabilities on outboard side

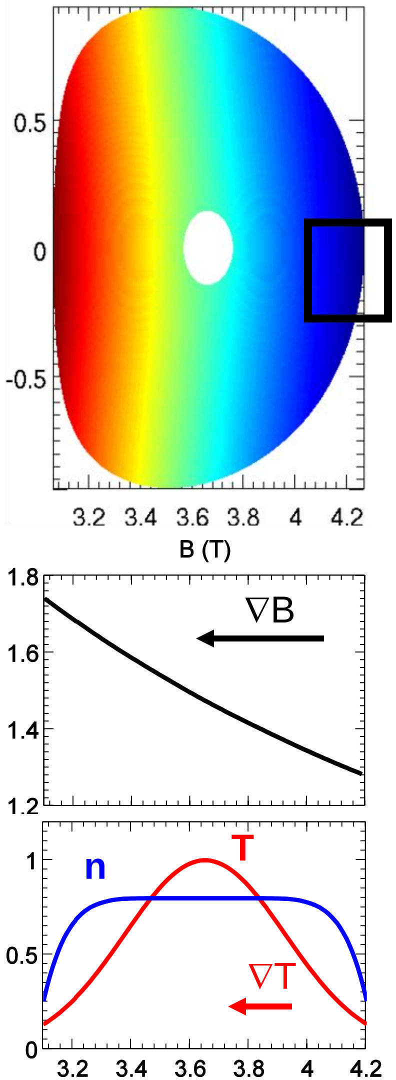

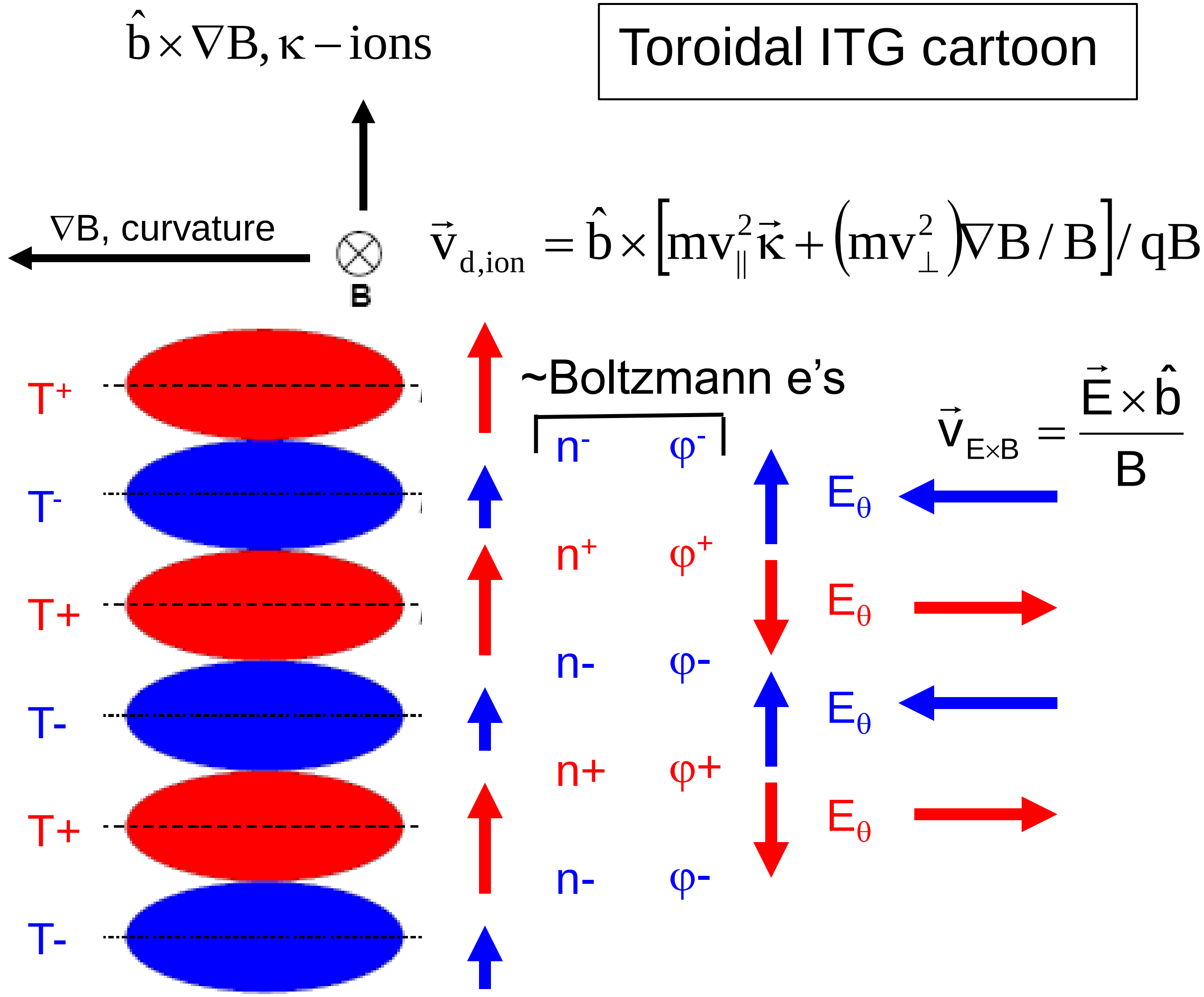

ITG/TEM & ETG turbulence appears to describe tokamak transport in many cases

Ion scales ($k_\perp \rho_i$~1)

- Ion temperature gradient (**ITG**, $\gamma \sim \nabla T_i$) via ion compressibility (~∇B, κ)
- Trapped electron mode (**TEM**, $\gamma \sim \nabla T_e, \nabla n_e$) from electron trapping (~f_t)

Electron scales ($k_\perp \rho_e$~1)

- Electron temperature gradient (**ETG**, $\gamma \sim \nabla T_e$), analogous to ITG (~∇B, κ)

- Instabilities driven by gradients (∇T_i, ∇T_e, ∇n) surpassing thresholds which depend on: connection length (~qR), magnetic shear (dq/dr), temperature ratio (T_e/T_i), additional equilibrium effects …

- NOTE: in this talk I am drawing heavily on gyrokinetic theory and simulation results

Many elements of ST are stabilizing to toroidal, electrostatic ITG/TEM drift waves

- Short connection length → **smaller average bad curvature**

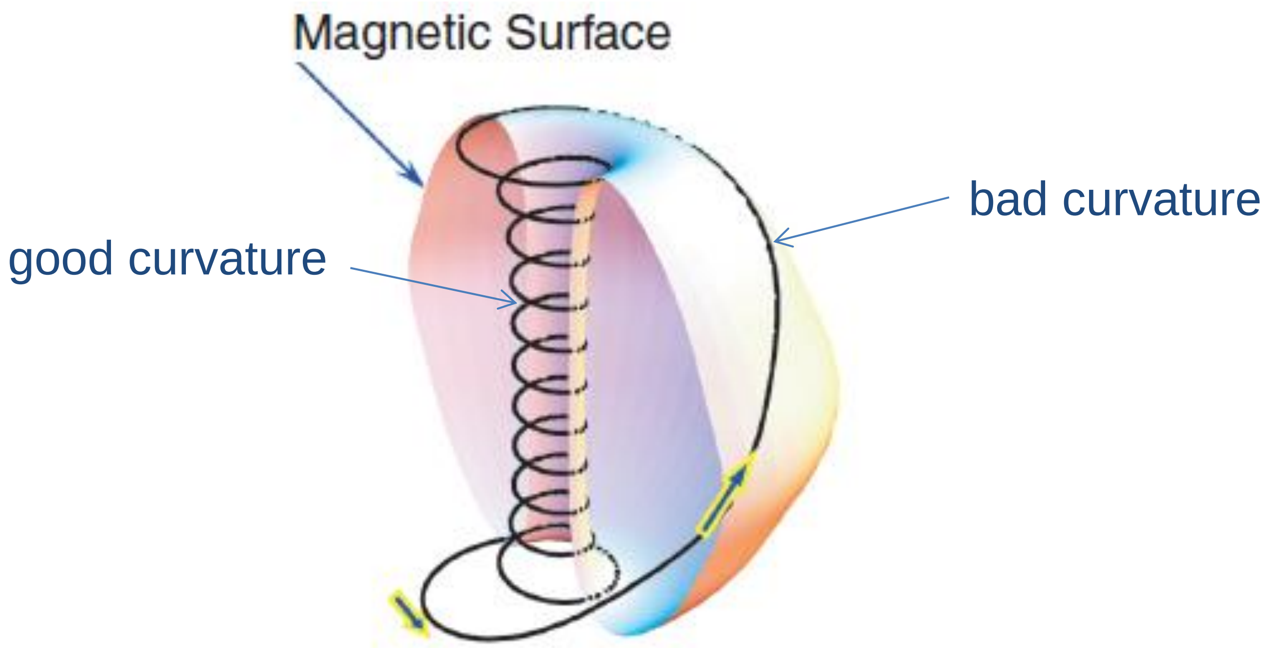

Many elements of ST are stabilizing to toroidal, electrostatic ITG/TEM drift waves

- Short connection length → **smaller average bad curvature**
- Quasi-isodynamic (~constant B) at high β → **grad-B drifts stabilizing [Peng & Strickler, NF 1986]**

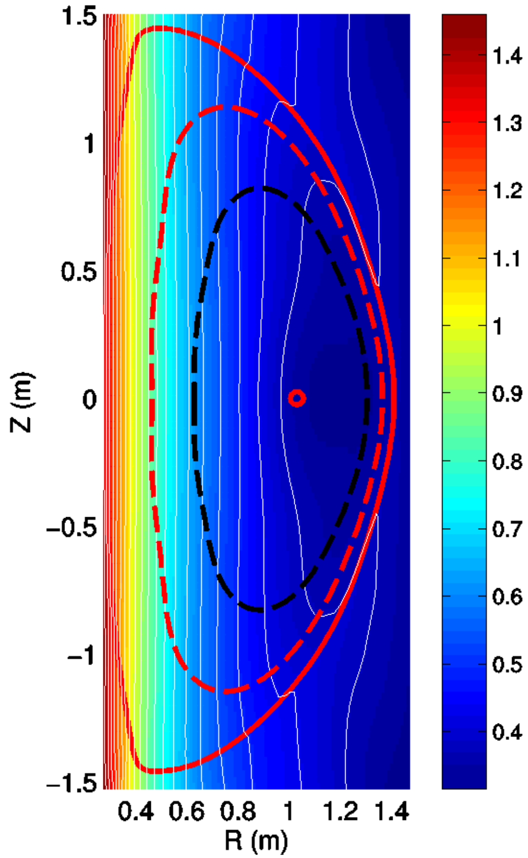

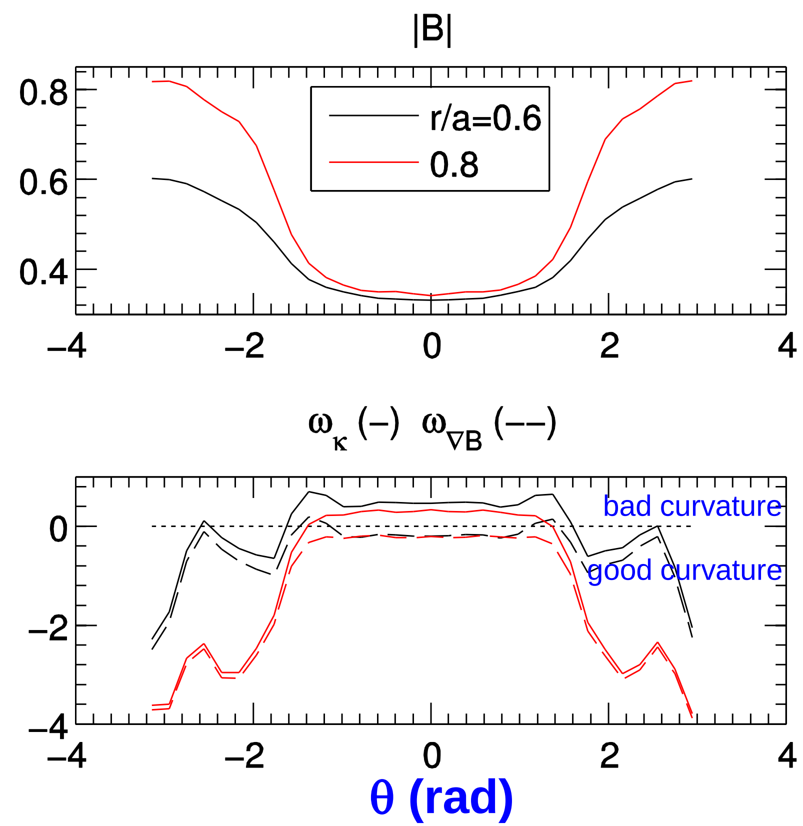

$$\vec{v}_{\kappa} = m v_{||}^2 \frac{\hat{b}\times\vec{\kappa}}{qB}$$

$$\vec{v}_{\nabla B} = \frac{m v_{\perp}^2}{2}\frac{\hat{b}\times\nabla B/B}{qB}$$

Many elements of ST are stabilizing to toroidal, electrostatic ITG/TEM drift waves

- Short connection length → **smaller average bad curvature**
- Quasi-isodynamic (~constant B) at high β → **grad-B drifts stabilizing [Peng & Strickler, NF 1986]**
- Large fraction of trapped electrons, BUT precession weaker at low A → **reduced TEM drive [Rewoldt, Phys. Plasmas 1996]**

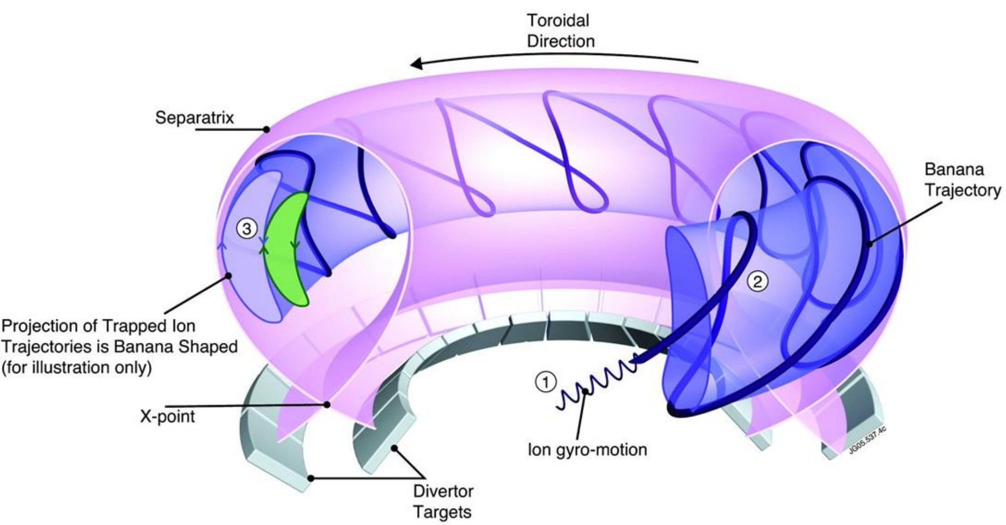

Orbit-averaged drift of trapped particle

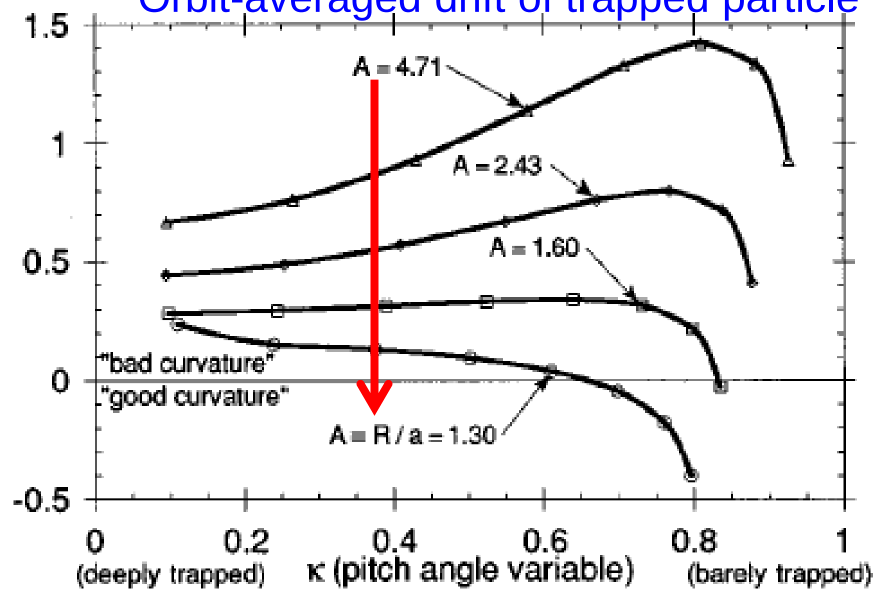

Many elements of ST are stabilizing to toroidal, electrostatic ITG/TEM drift waves

- Short connection length → **smaller average bad curvature**
- Quasi-isodynamic (~constant B) at high β → **grad-B drifts stabilizing [Peng & Strickler, NF 1986]**
- Large fraction of trapped electrons, BUT precession weaker at low A → **reduced TEM drive [Rewoldt, Phys. Plasmas 1996]**
- Strong coupling to $\delta B_\perp \sim \delta A_{||}$ at high β → **stabilizing to ES-ITG**

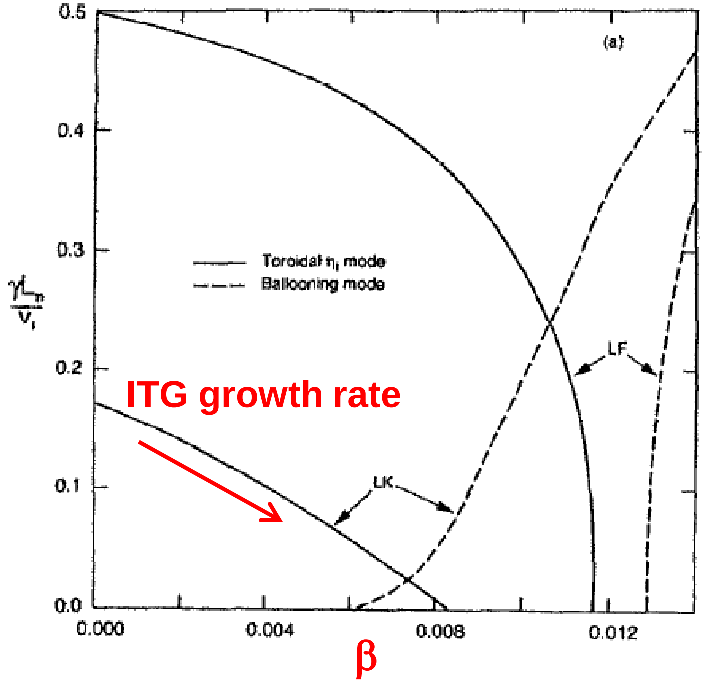

Kim, Horton, Dong, PoFB (1993)

Many elements of ST are stabilizing to toroidal, electrostatic ITG/TEM drift waves

- Short connection length → **smaller average bad curvature**
- Quasi-isodynamic (~constant B) at high β → **grad-B drifts stabilizing [Peng & Strickler, NF 1986]**
- Large fraction of trapped electrons, BUT precession weaker at low A → **reduced TEM drive [Rewoldt, Phys. Plasmas 1996]**
- Strong coupling to $\delta B_\perp \sim \delta A_\parallel$ at high β → **stabilizing to ES-ITG**
- Small inertia ($nm\underline{R}^2$) with uni-directional NBI heating gives strong toroidal flow & flow shear → **E×B shear stabilization ($dv_\perp/dr$)**

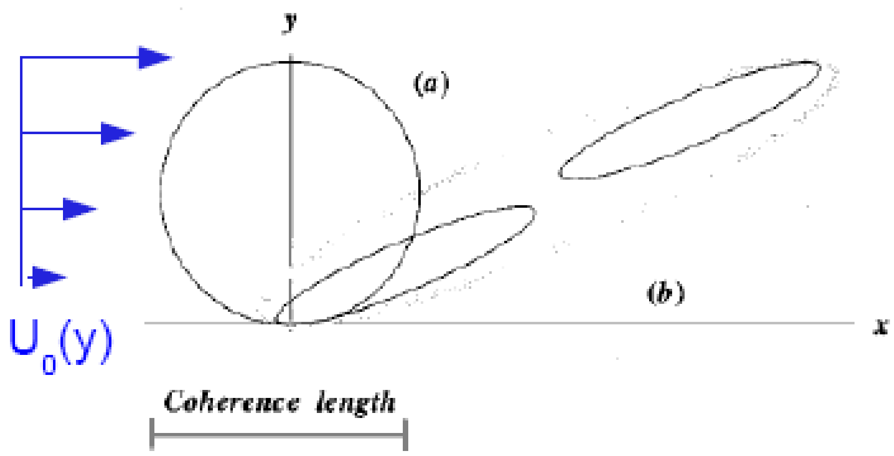

Biglari, Diamond, Terry, PoFB (1990)

Many elements of ST are stabilizing to toroidal, electrostatic ITG/TEM drift waves

- Short connection length → **smaller average bad curvature**
- Quasi-isodynamic (~constant B) at high β → **grad-B drifts stabilizing [Peng & Strickler, NF 1986]**
- Large fraction of trapped electrons, BUT precession weaker at low A → **reduced TEM drive [Rewoldt, Phys. Plasmas 1996]**
- Strong coupling to $\delta B_\perp \sim \delta A_{||}$ at high β → **stabilizing to ES-ITG**
- Small inertia (nmR^2) with uni-directional NBI heating gives strong toroidal flow & flow shear → **E×B shear stabilization ($dv_\perp/dr$)**

⇒**Not expecting strong ES ITG/TEM instability (much higher thresholds)**

- <u>BUT</u>
- High beta drives EM instabilities: microtearing modes (**MTM**) ~ $\beta_e \cdot \nabla T_e$, kinetic ballooning modes (**KBM**) ~ $\alpha_{MHD} \sim q^2 \nabla P/B^2$
- Large shear in parallel velocity can drive Kelvin-Helmholtz-like instability $\sim dv_{||}/dr$

NSTX (1999-2010)

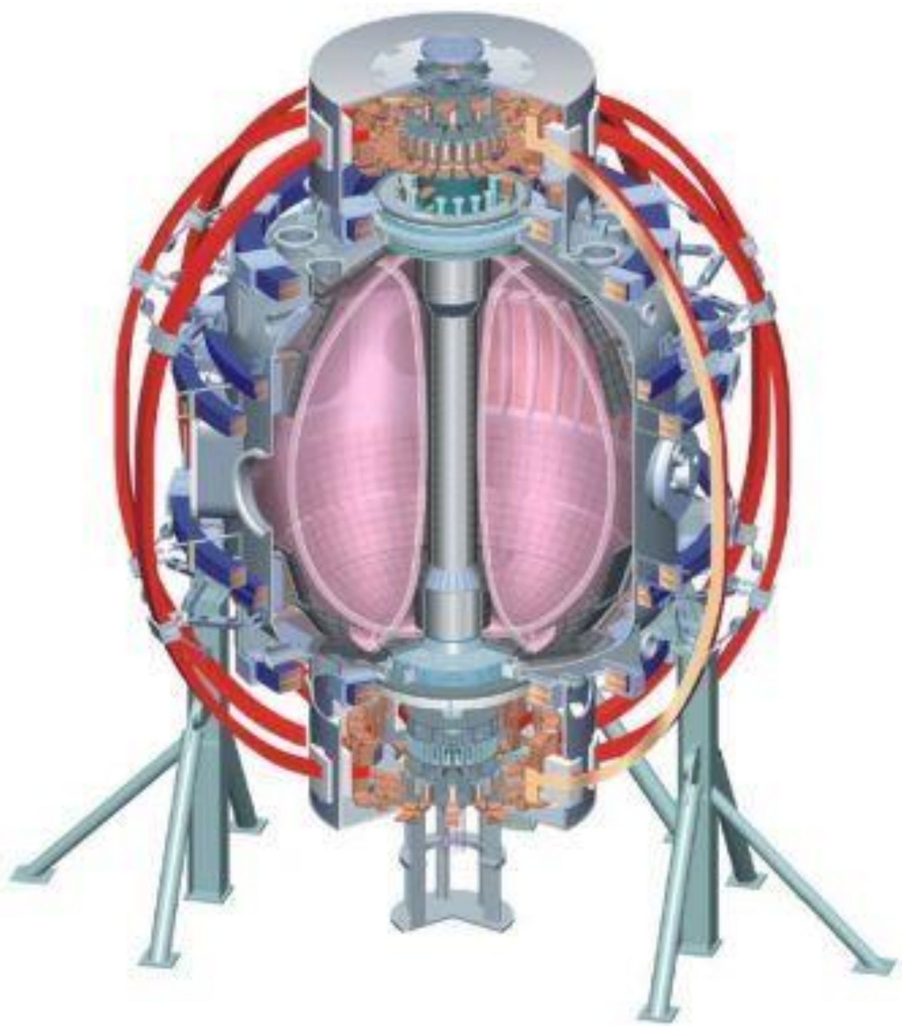

R	~0.9 m
a	~0.6 m
B_{tor}	$\leq$ 0.55 T
I_p	$\leq$ 1.3 MA
P_{NBI}/P_{RF}	$\leq$ 7 MW / 3 MW
β_{tor}	$\leq$ 40%
Pulse length	$\leq$ 2 s

- Graphite PFCs
- Lithium evaporation was available to condition lower divertor region

Ion thermal transport in H-modes (higher beta) usually very close to collisional (neoclassical) transport theory

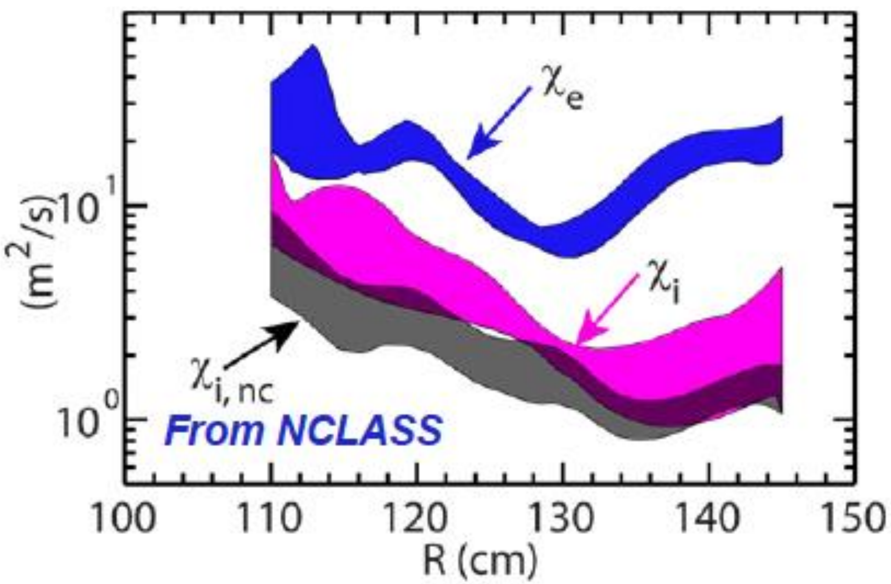

Courtesy Y. Ren

- Consistent with ITG/TEM stabilization by equilibrium configuration & strong E×B flow shear
  – Impurity transport (intrinsic carbon, injected Ne, …) also usually well described by neoclassical theory [Delgado-Aparicio, NF 2009 & 2011 ; Scotti, NF 2013]

- **Electron energy transport always anomalous**
  – Toroidal angular momentum transport also anomalous (Kaye, NF 2009)

Unique Ip, BT confinement scaling, depending on wall conditioning

- $\tau_E \sim I_p^{0.4} B_T^{1.0}$ (boronization + between-shots He GDC)
- $\tau_E \sim I_p^{0.8} B_T^{-0.15}$ (between-shots Lithium evap.) – similar to ITER $\tau_{E,98y2} \sim I_p^{0.9} B_T^{-0.15}$
- Differences in profile shapes, ELM behavior, impurity content

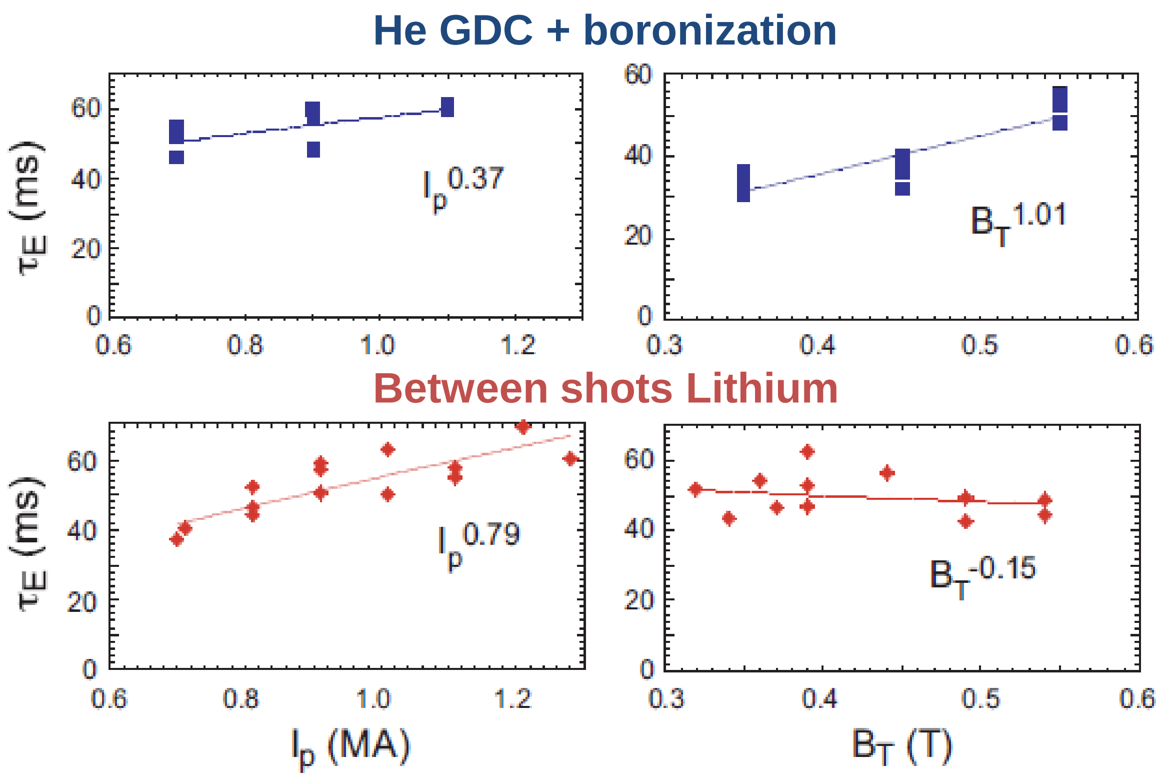

Kaye, NF (2007)
PRL (2007)
NF (2013)

Normalized energy confinement time scales favorably with collisionality in STs

- $\tau_E \sim I_p^{0.4} B_T^{1.0}$ (boronization + between-shots He GDC)
- $\tau_E \sim I_p^{0.8} B_T^{-0.15}$ (between-shots Lithium evap.) – similar to ITER $\tau_{E,98y2} \sim I_p^{0.9} B_T^{-0.15}$
- Differences in profile shapes, ELM behavior, impurity content

- Considering dimensionless scaling ($\sim\rho_*$, q, β, ν_*), $\mathbf{\Omega_{ci}\tau_E \sim \nu_*^{-0.8}\, \beta^{0.0}}$
- Next generation STs (FNSF, CTF, Pilot Plant) likely to be at lower ν_*
  – Will favorable ν_* scaling continue?
  – Hints at lower ν_* that $\chi_i > \chi_{i,NC}$

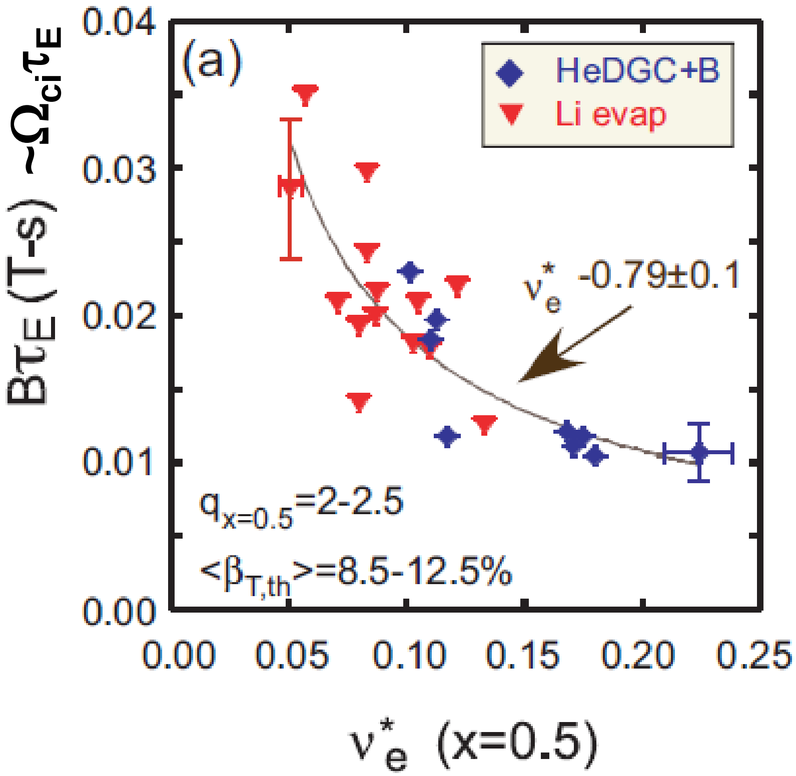

Kaye, NF (2013)

Going to consider three regions of the plasma

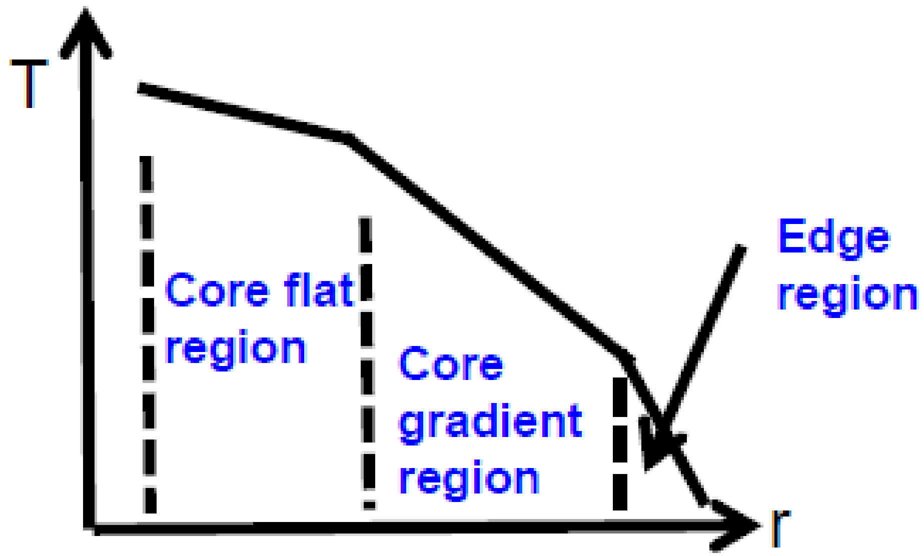

- H-mode edge pedestal – strong gradients
- Core gradient region – inside pedestal
- Core flat region – region of weak ∇Te

} Susceptible to gradient-driven instabilities (e.g. drift-waves)

} Must consider other mechanisms (e.g. driven by fast-ions)

Going to consider three regions of the plasma

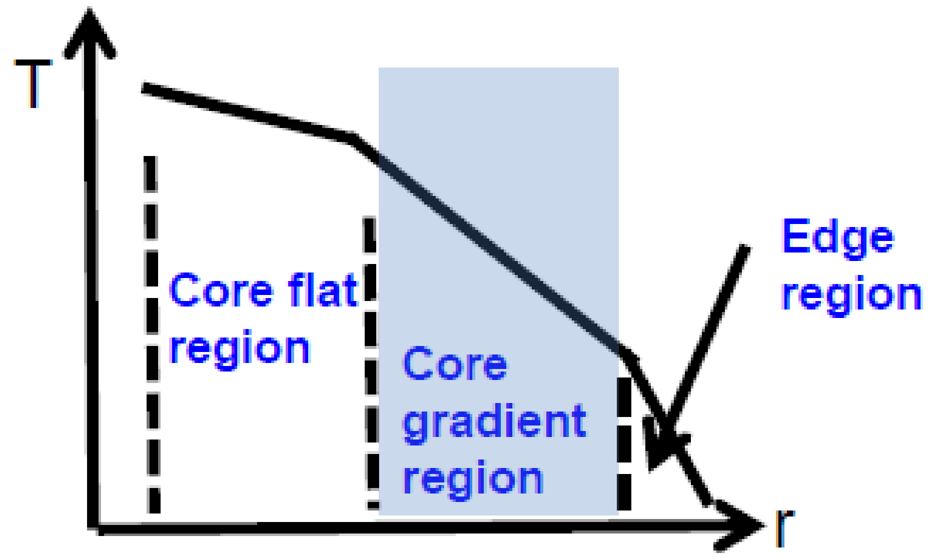

- H-mode edge pedestal – strong gradients
- Core gradient region – inside pedestal
- Core flat region – region of weak ∇Te

} Susceptible to gradient-driven instabilities (e.g. drift-waves)

} Must consider other mechanisms (e.g. driven by fast-ions)

Predicted dominant core-gradient instability correlated with local beta and collisionality

- For sufficiently small β, ES instabilities can exist (ITG, TEM, ETG)
- At increasing β, MTM and KBM are predicted → depending on ν
  - Various instabilities often predicted in the same discharge – global, nonlinear EM theory & predictions will hopefully simplify interpretation (*under development*)

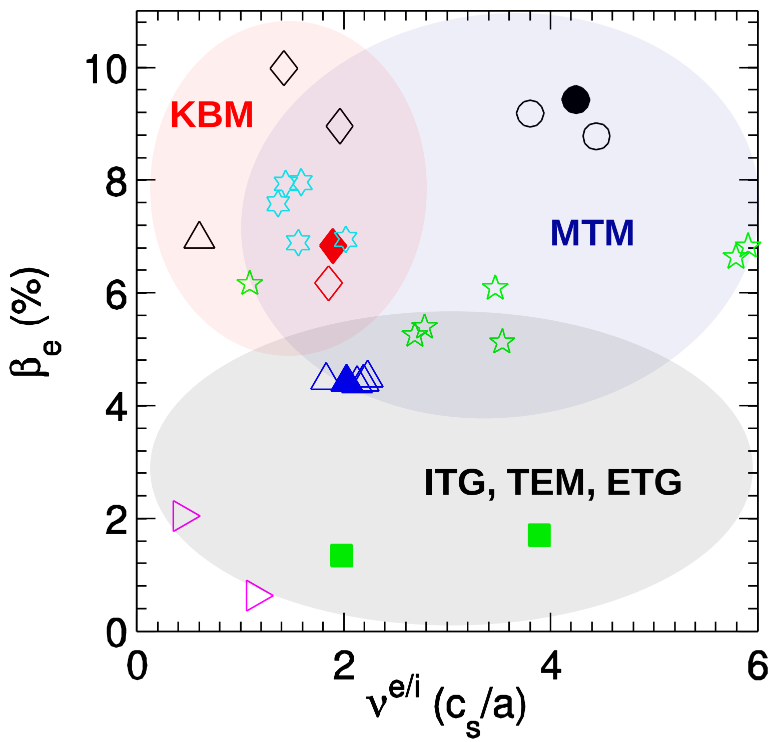

Guttenfelder, NF (2013)

Local gyrokinetic analyses at ~2/3 radius

Simulations of core microtearing mode (MTM) turbulence predict significant transport at high β & ν

- Collisionality scaling ($\chi_{e,MTM} \sim \nu_e$) consistent with global confinement ($\tau_E \sim 1/\nu$), follows linear stability trends:
  - In the core, driven by ∇T_e with time-dependent thermal force (e.g. Hassam, 1980)
  - *Requires collisionality $\rightarrow$* ***not explicitly driven by bad-curvature***

Predicted transport

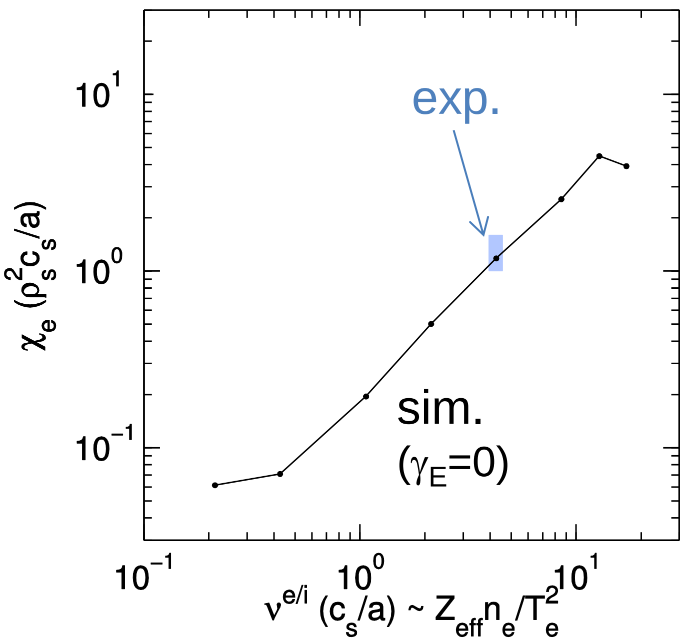

Guttenfelder, PRL (2011), PoP (2012)

Simulations of core microtearing mode (MTM) turbulence predict significant transport at high β & ν

- Collisionality scaling ($\chi_{e,MTM} \sim \nu_e$) consistent with global confinement ($\tau_E \sim 1/\nu$), follows linear stability trends:
  - In the core, driven by ∇T_e with time-dependent thermal force (e.g. Hassam, 1980)
  - *Requires collisionality* $\rightarrow$ ***not explicitly driven by bad-curvature***
- δB leads to flutter transport ($\sim v_{\|} \cdot \delta B^2$) consistent with stochastic transport

Predicted transport

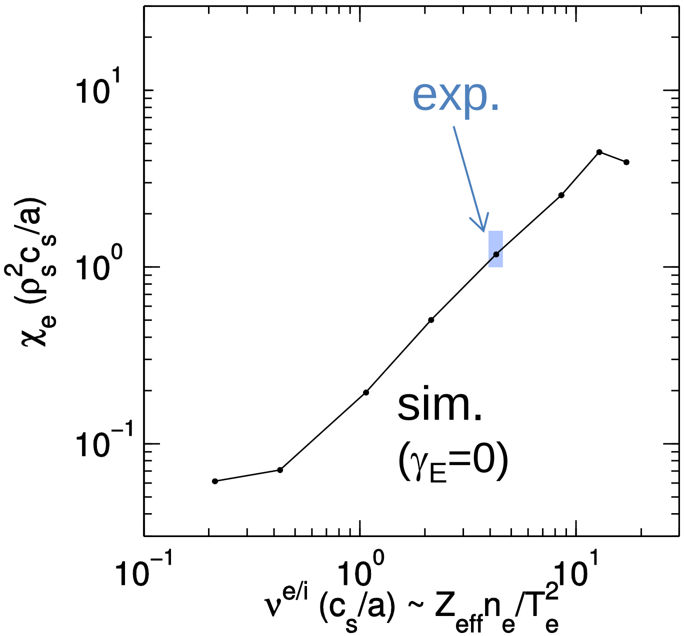

Guttenfelder, PRL (2011), PoP (2012)

Poincare plots of flux-tube surfaces

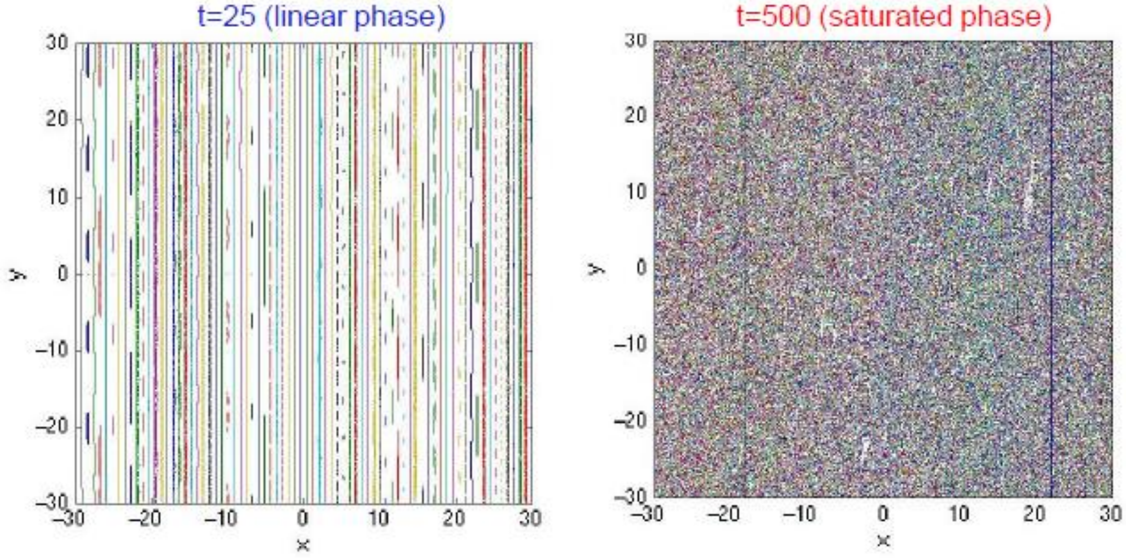

E. Wang, PoP (2011)

MTM structure distinct from ballooning modes

Predictions from MTM simulation

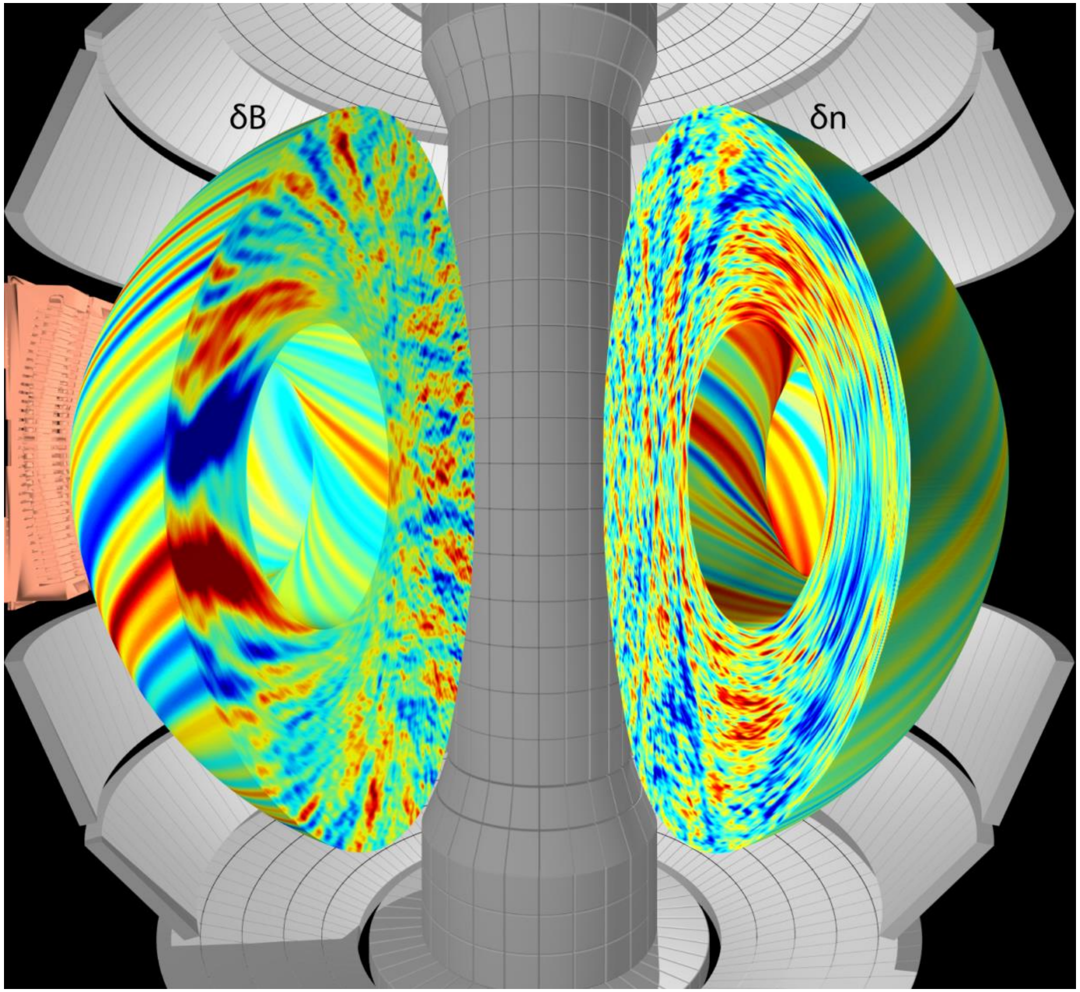

Visualization courtesy F. Scotti (LLNL)

- Narrow density perturbations due to high-m tearing mode around rational surfaces q=m/n
  – Potential to validate with beam emission spectroscopy (BES) imaging [Smith, RSI (2012)]
- Large $\delta B/B \sim 10^{-3}$
  – Potential for internal δB measurements via cross polarization scattering (UCLA collaboration)

At high β & lower ν, KBM modes predicted; Sensitive to compressional magnetic ($B_{||}$) perturbations

- Kinetic analogue of MHD high-n ballooning mode, driven by total ∇P (α_{MHD})
- Smooth transition from ITG/TEM at reduced ∇P
- Transport has significant compressional component ($\sim\delta B_{||}$)

Linear growth rates

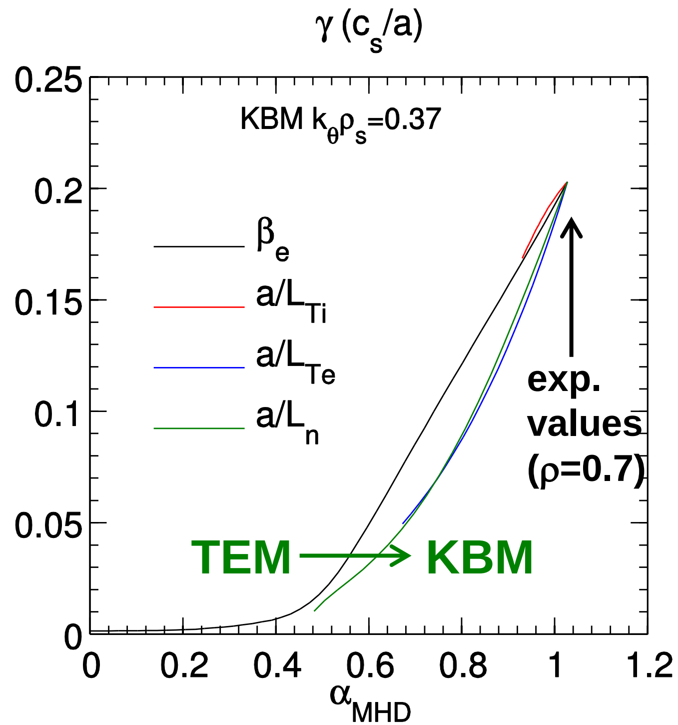

$$\alpha_{MHD} = -q^2 R \cdot 2\mu_0 \nabla P / B^2$$

Guttenfelder, NF (2013)

Electron scale turbulence measured and predicted at lower beta

"Microwave scattering" used to detect high-$k_\perp$ (~mm) fluctuations

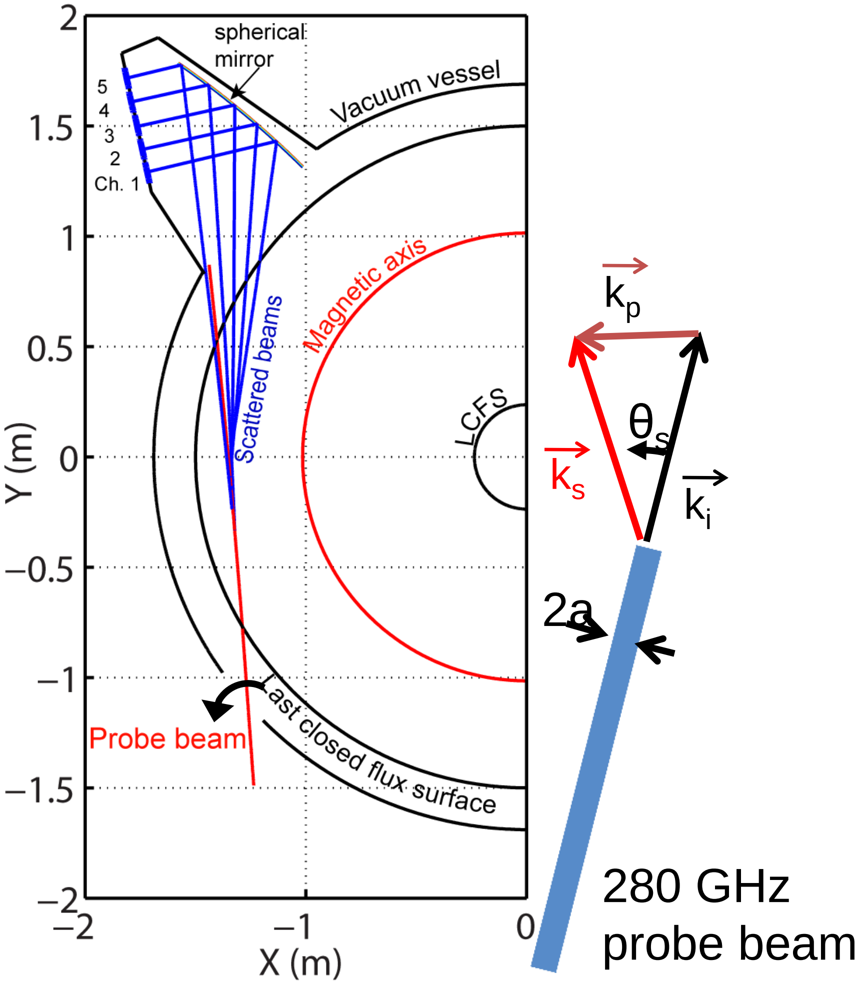

Mazzucato, PRL (2008)
Smith, RSI (2008)

density fluctuations from ETG simulation

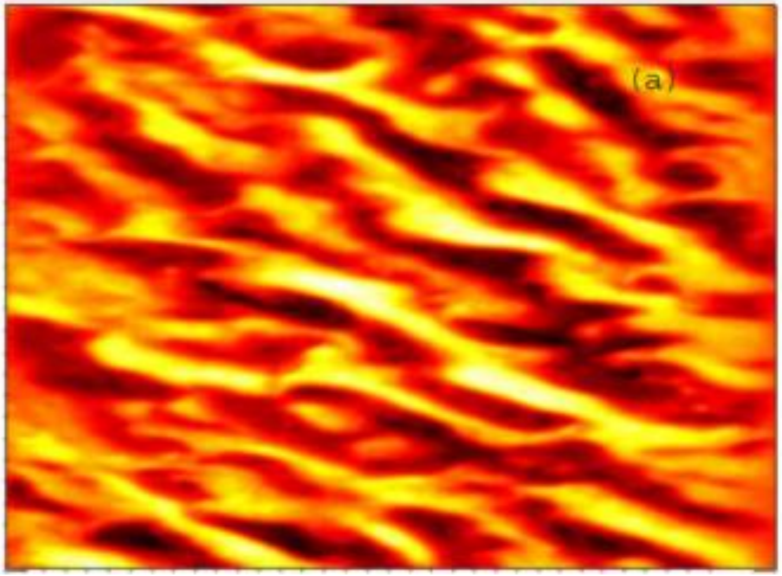

6 ion radii
360 electron radii
~2 cm

Guttenfelder, PoP (2011)

Correlation observed between high-k scattering fluctuations and ∇T_e

- Applying RF heating to increase Te
- Fluctuations increase as expected for ETG turbulence ($R/L_{Te} > R/L_{Te,crit}$)

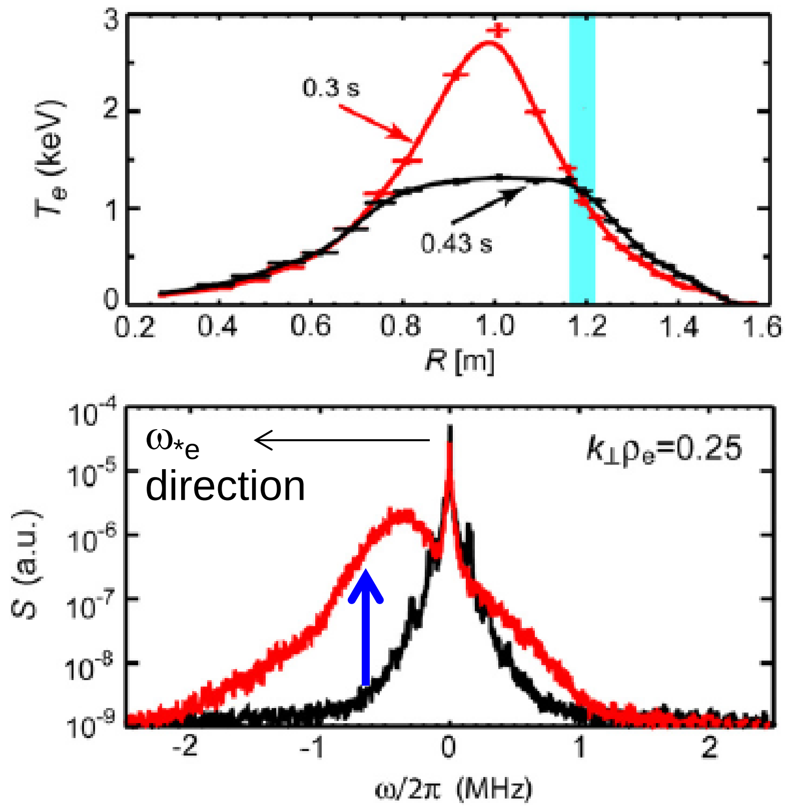

E. Mazzucato et al., NF (2009)

Correlation observed between high-k scattering fluctuations and ∇T_e

- Applying RF heating to increase Te
- Fluctuations increase as expected for ETG turbulence ($R/L_{Te} > R/L_{Te,crit}$)

- Other trends measured that are consistent with ETG expectations, e.g. reduction of high-k scattering fluctuations with:

1. Strongly reversed magnetic shear (Yuh, PRL 2011)
   – Simulations predict comparable suppression (Peterson, PoP 2012)
2. Increasing density gradient (Ren, PRL 2011)
   – Simulations predict comparable trend (Ren, PoP 2012, Guttenfelder NF, 2013, Ruiz PoP 2015)
3. Sufficiently large E×B shear (Smith, PRL 2009)
   – Observed in ETG simulations (Roach, PPCF 2009; Guttenfelder, PoP 2011)

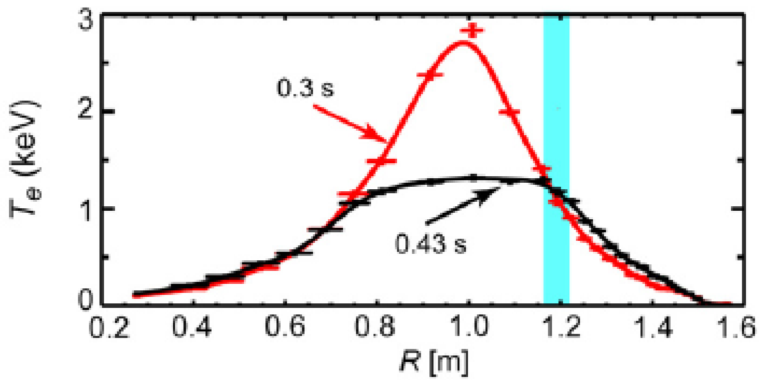

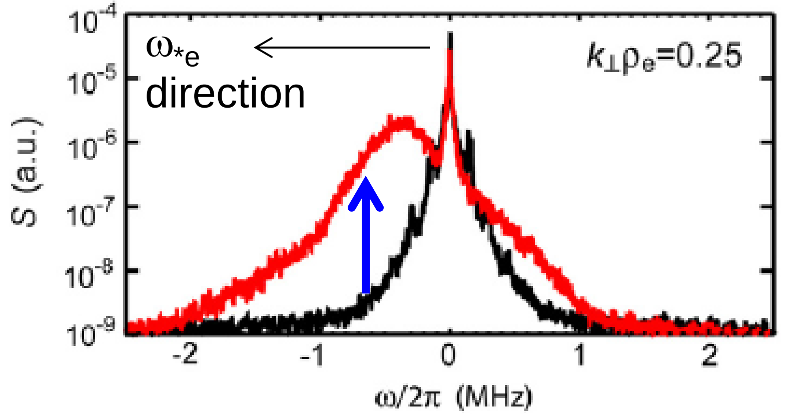

E. Mazzucato et al., NF (2009)

While many high-k trends correlate with ETG predictions, predicted transport not always sufficient

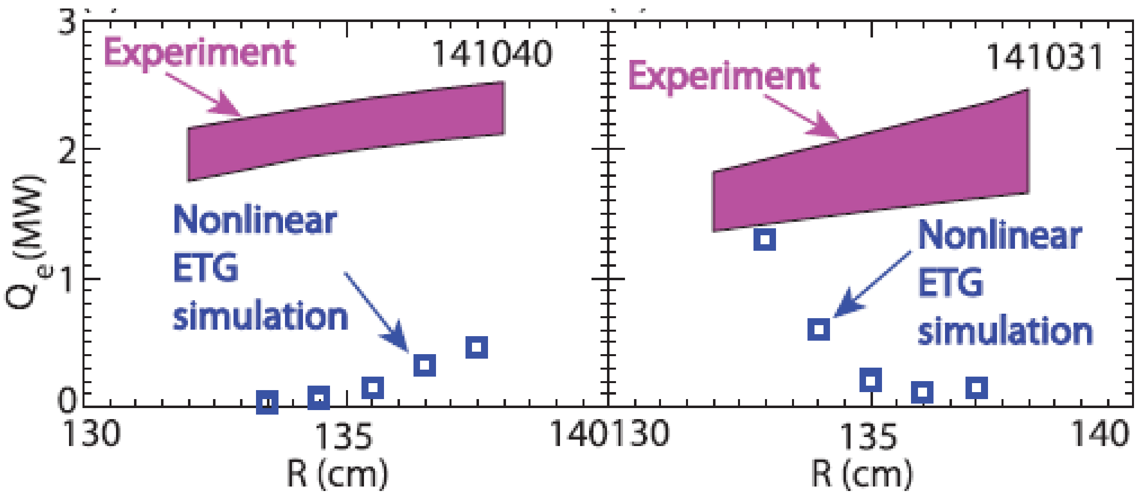

Ren, PoP (2012)

Simulated ETG spectra

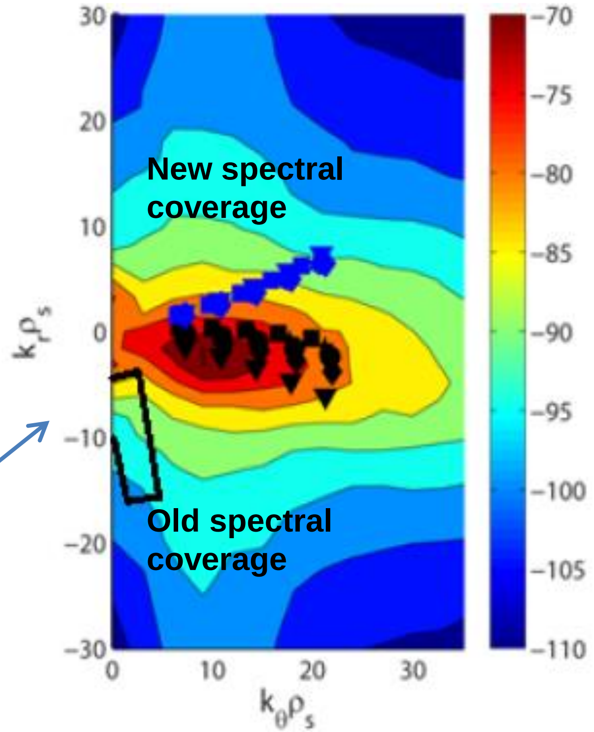

- May require multi-scale simulations spanning ρ_i to ρ_e (e.g. N. Howard, NF 2016)
- New high-k scattering configuration should allow improved spectral coverage
  - Will allow more direct validation of streamer-like ETG structure ($k_\theta >> k_r$)

H-mode edge pedestal is important in setting global confinement

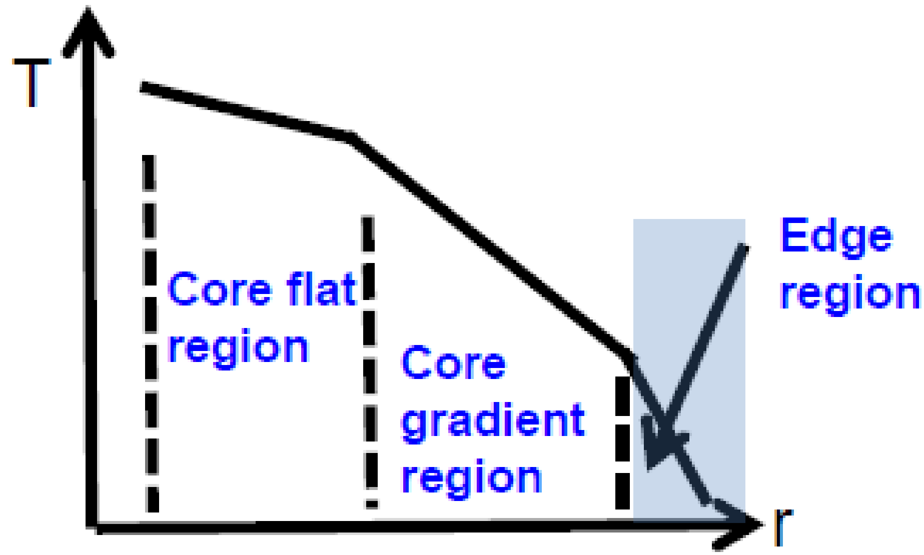

- **Similar drift wave instabilities predicted in the H-mode edge pedestal**

Example: H-mode pedestal influenced by Lithium wall conditioning

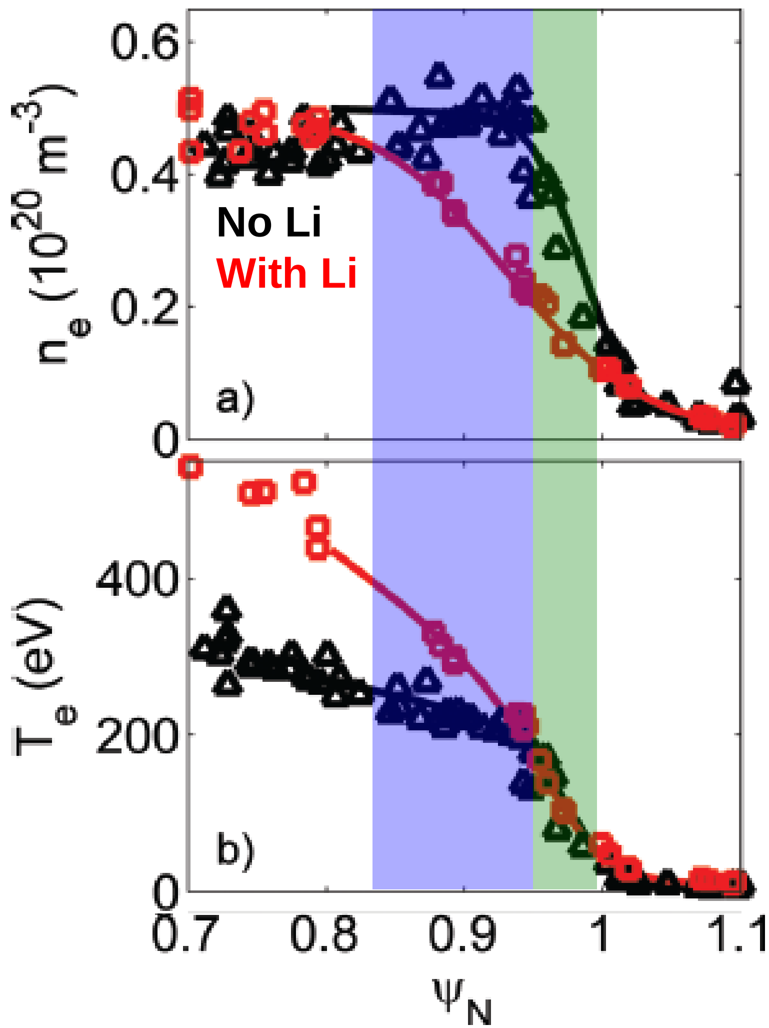

Canik, PoP (2011)

- Depositing lithium between shots leads to reduced ∇n, increased ∇T (ψ_N<0.95), improved confinement (& eliminates ELMs)
- Inside ψ_N<0.95, increased ∇n predicted to be stabilizing to MTM (consistent with reduced χ_e)

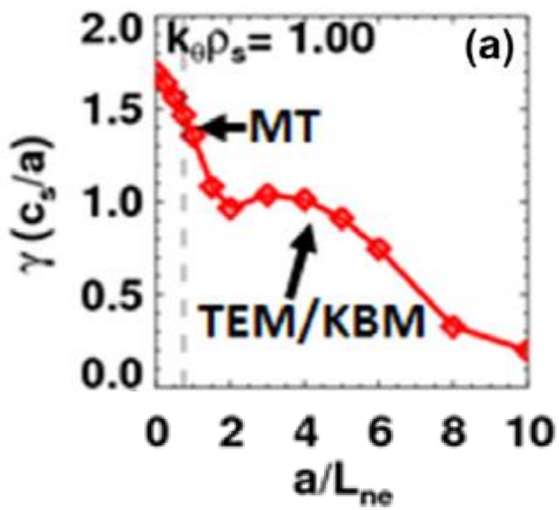

- Outside ψ_N>0.95, decreased ∇n destabilizing to ETG (~fixed ∇T_e)

Canik, NF (2013)

Non drift wave mechanisms may also influence thermal transport

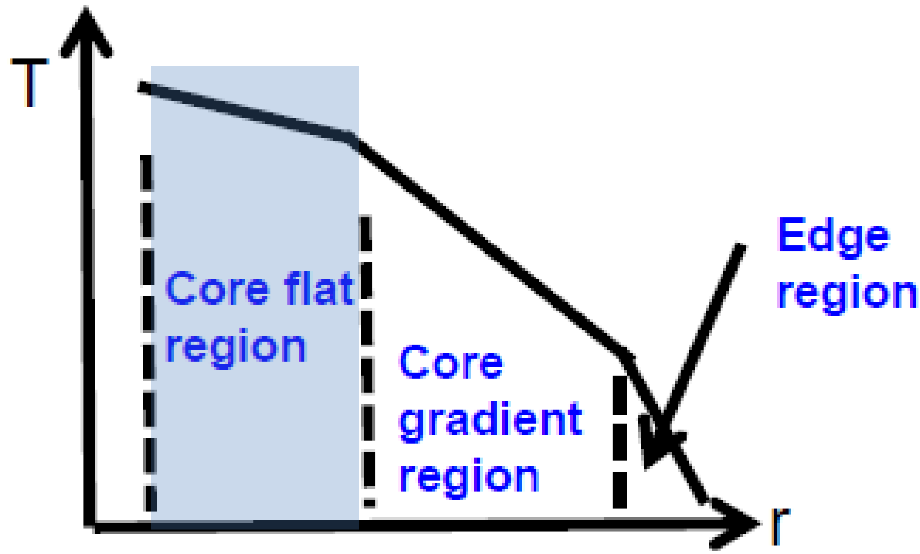

Max T_e limited in high power H-modes,

- Thermal-gradient-driven microinstabilities unlikely to explain flattened profiles
  - **Unless substantial non-local effects (~ρ_*) are important**

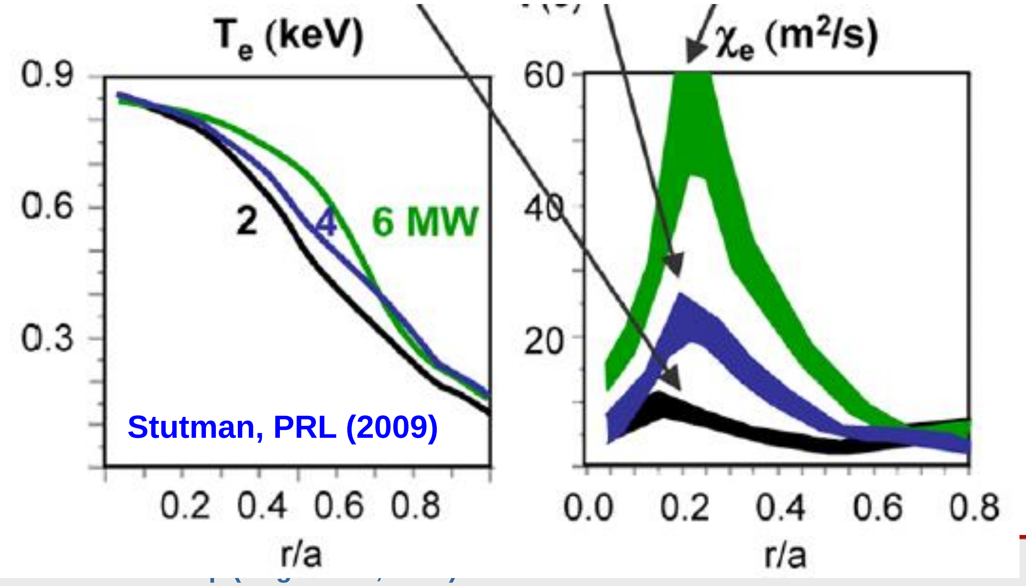

Max T_e limited in high power H-modes, correlated with presence of Global Alfven eigenmodes (GAE)

- Thermal-gradient-driven microinstabilities unlikely to explain flattened profiles
  - **Unless substantial non-local effects (~ρ_*) are important**
- High-frequency (ω/Ω_{ci}<1) Global/Compressional Alfven eigenmodes (GAE/CAE) measured [Crocker, NF 2013] and predicted [Belova, PRL 2015]
  - **Driven unstable by gradients in fast-ion phase space**
- **How do they influence electron thermal transport?**

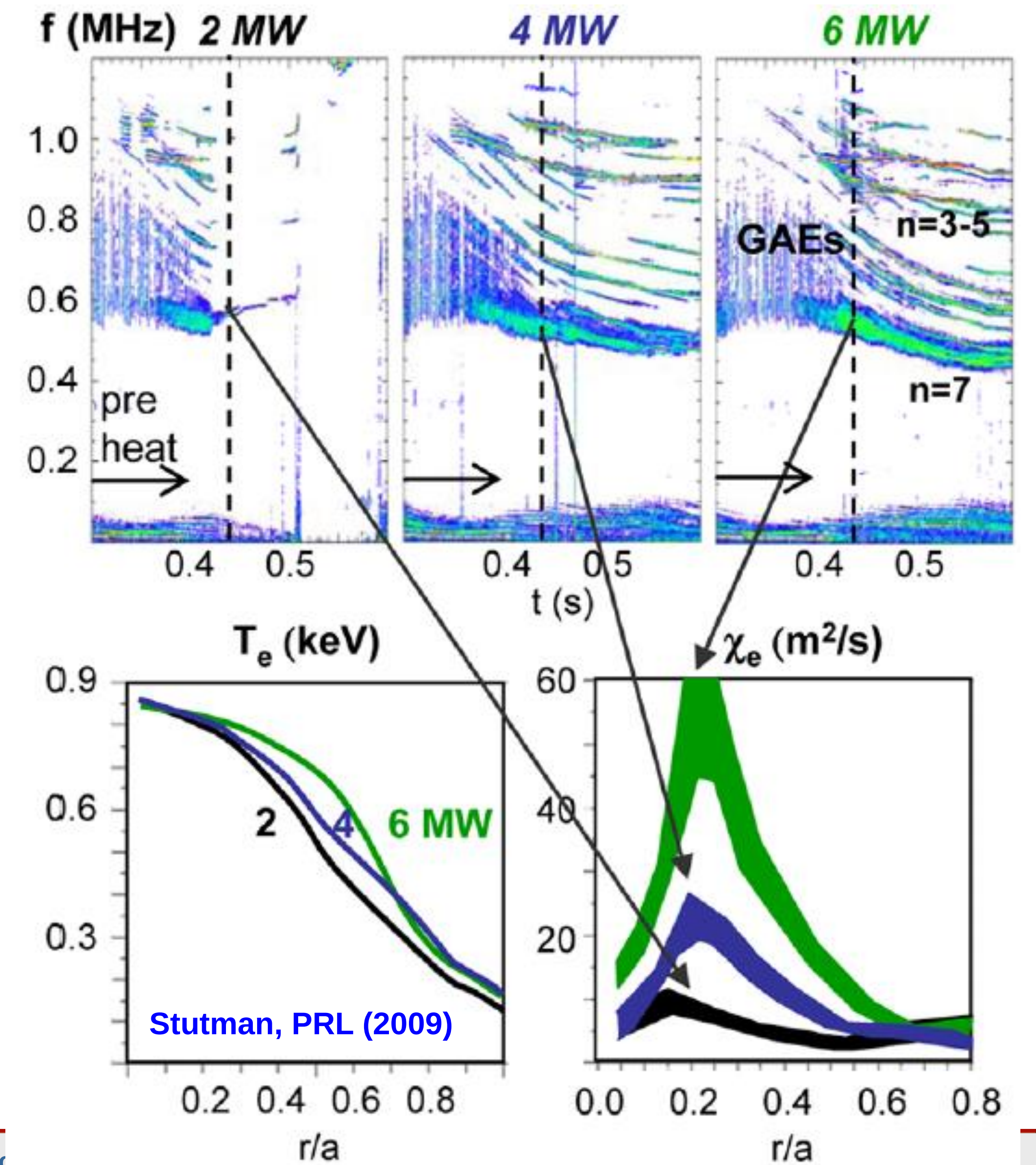

The presence of a large number of GAE/CAEs can stochasticize electron orbits

- Computed electron orbits become stochastic with sufficient number & amplitude of overlapping GAE & CAE modes [Gorelenkov, NF 2010]
- Stochastic orbits can give very large $\chi_{e,st} \sim \langle \Delta r^2 \rangle / \Delta t$

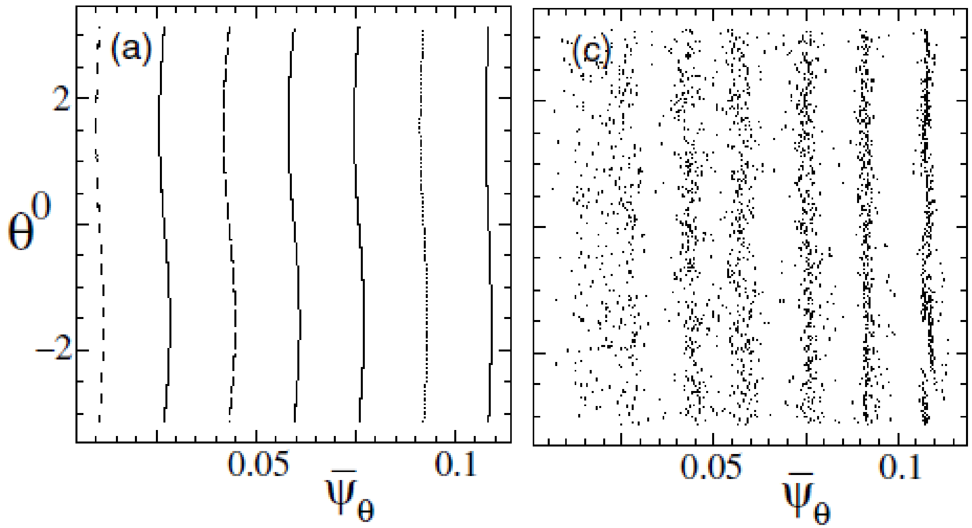

Gorelenkov, NF (2010); Crocker (2016)

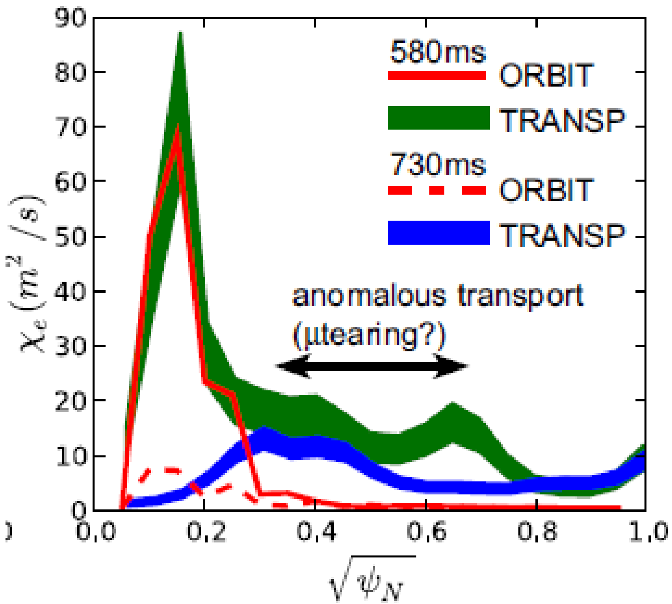

Tritz, APS (2012)

- CAE's also couple to kinetic Alfven waves (KAWs) near mid-radius → redistributes fast-ion energy to KAWs that damp on thermal electrons [Belova, PRL 2015]

NSTX-U

NSTX completed major upgrade in 2015 with goal of: 2 × higher B_T, I_p, P_{NBI} & 5 × longer pulse length

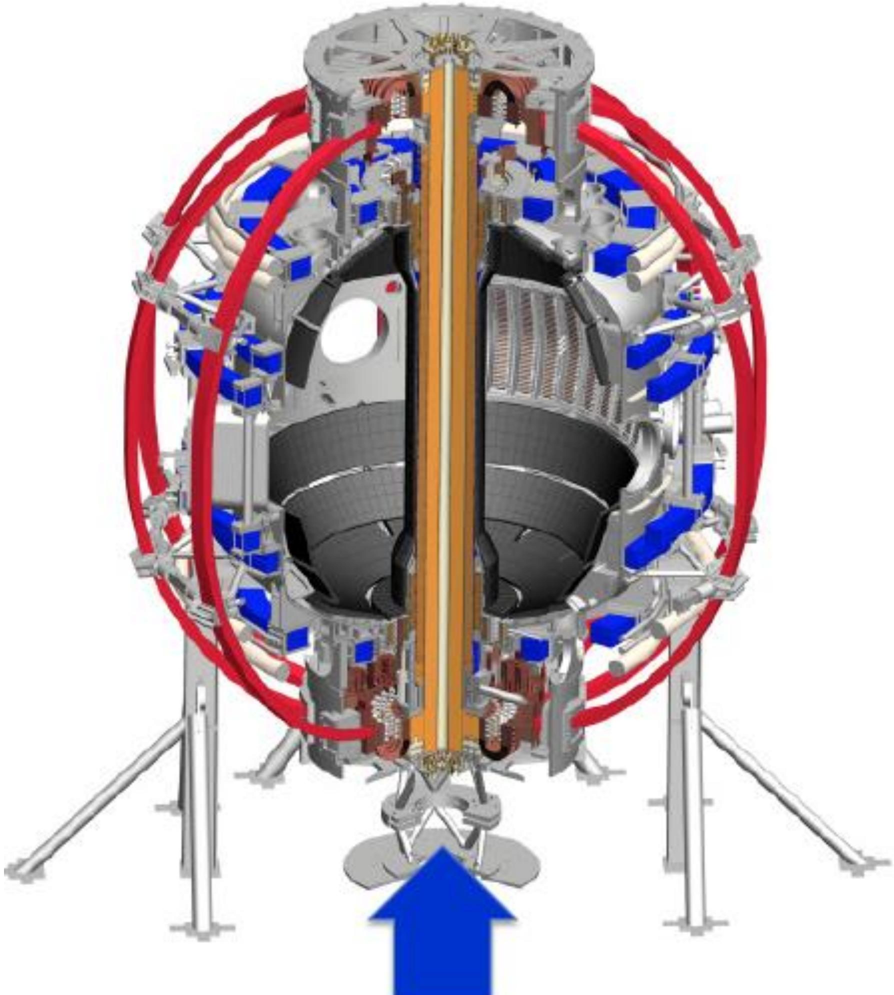

New Central Magnet

1 Tesla at plasma center, I_p = 2MA, 5s

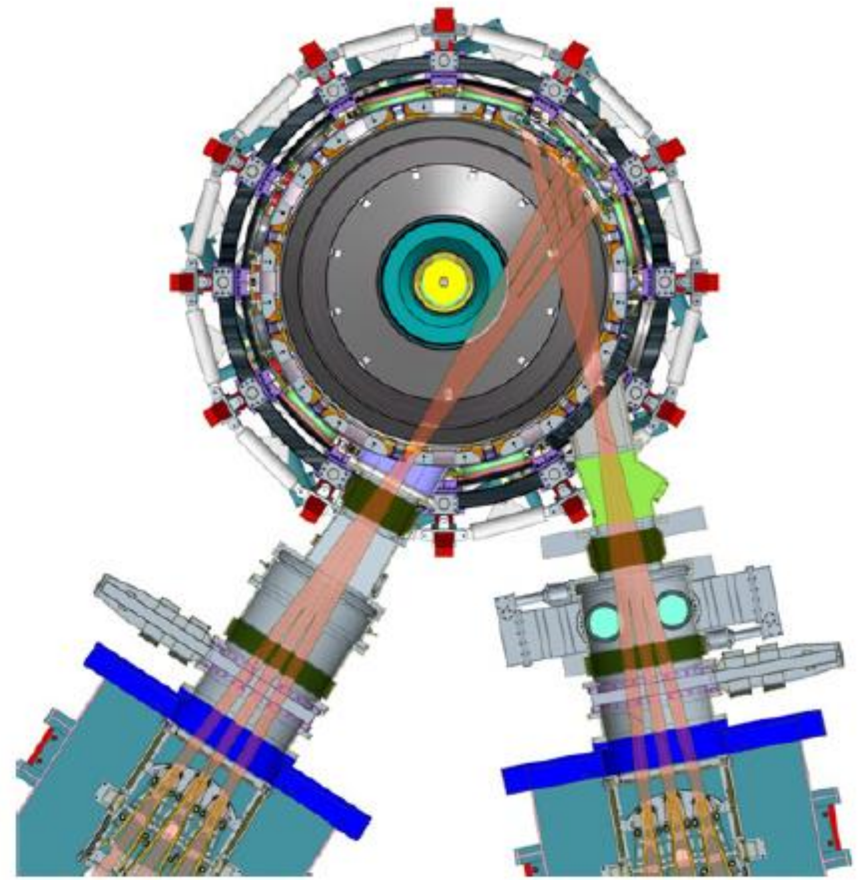

Original NBI

(R_{TAN} = 50, 60, 70cm)

5MW, 5s, 80keV

New 2nd NBI

(R_{TAN}=110, 120, 130cm)

5MW, 5s, 80keV

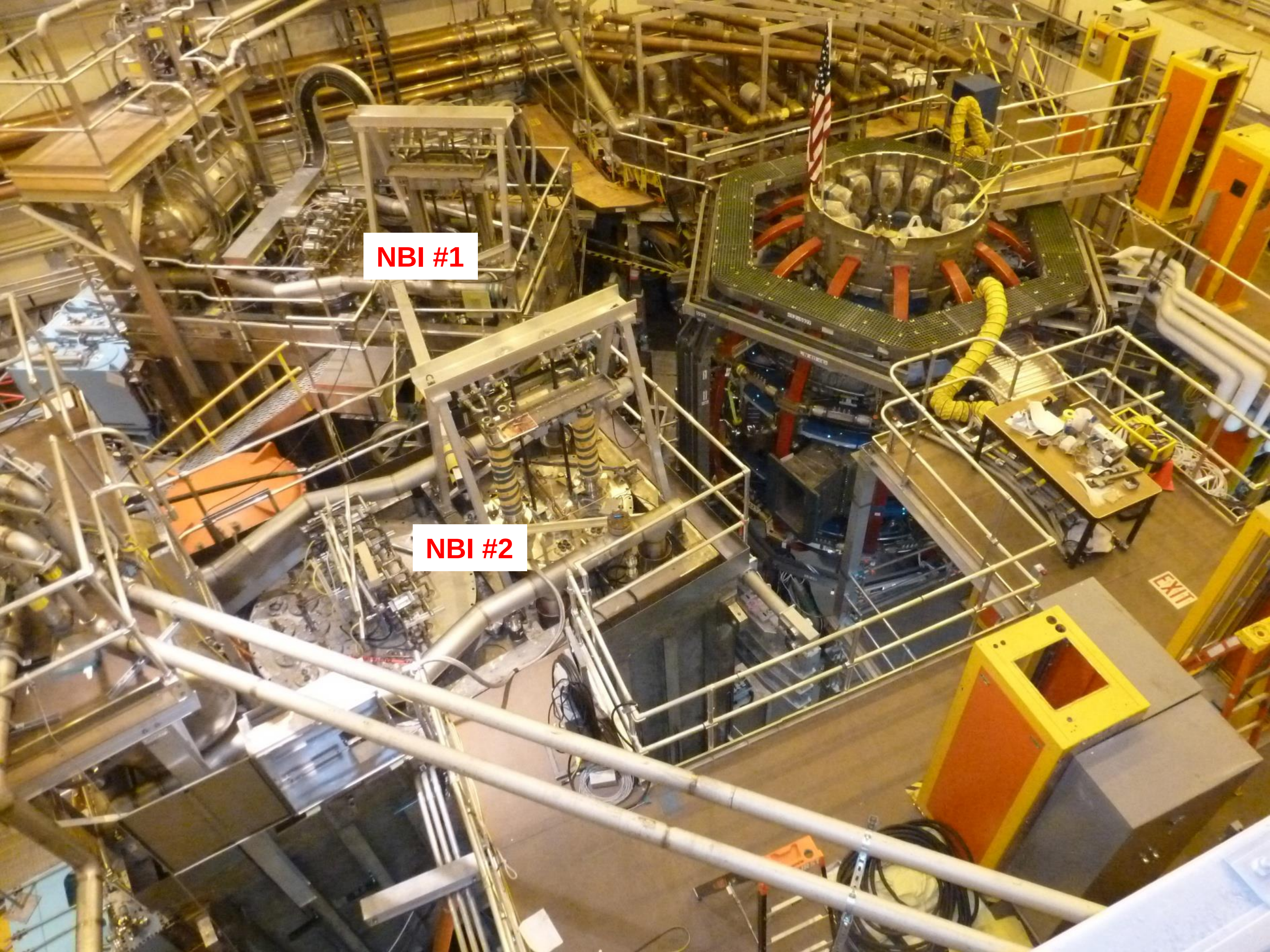
NBI #1
NBI #2

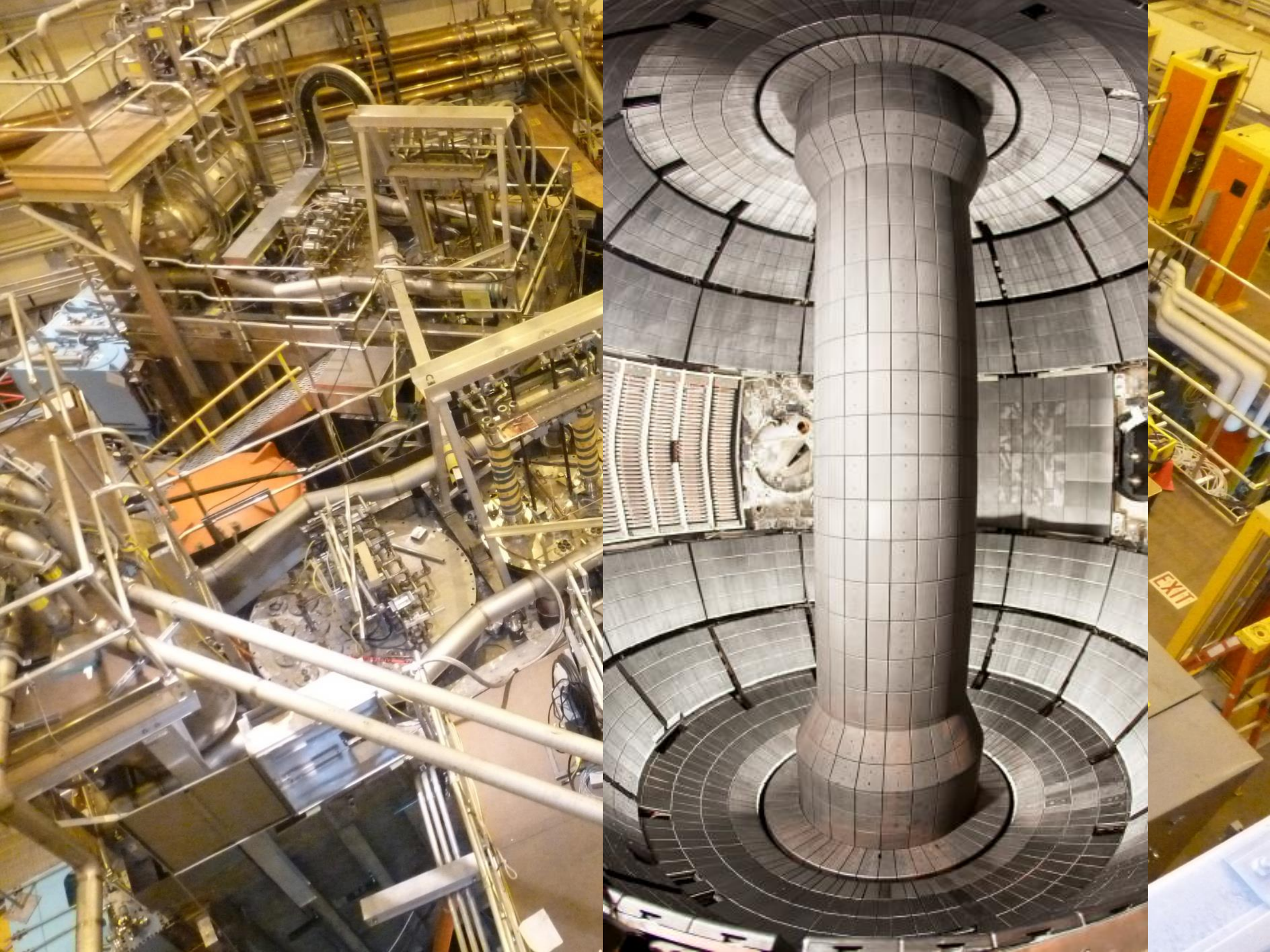
EXIT

NSTX-U recently completed its first experimental campaign

- First plasma August, 2015
  - Signified completion of major construction
- First experimental run from January to June, 2016
  - Focus was commissioning control, heating and diagnostic systems
- Next campaign slated to begin Spring of 2017
  - New capabilities, including lithium wall conditioning

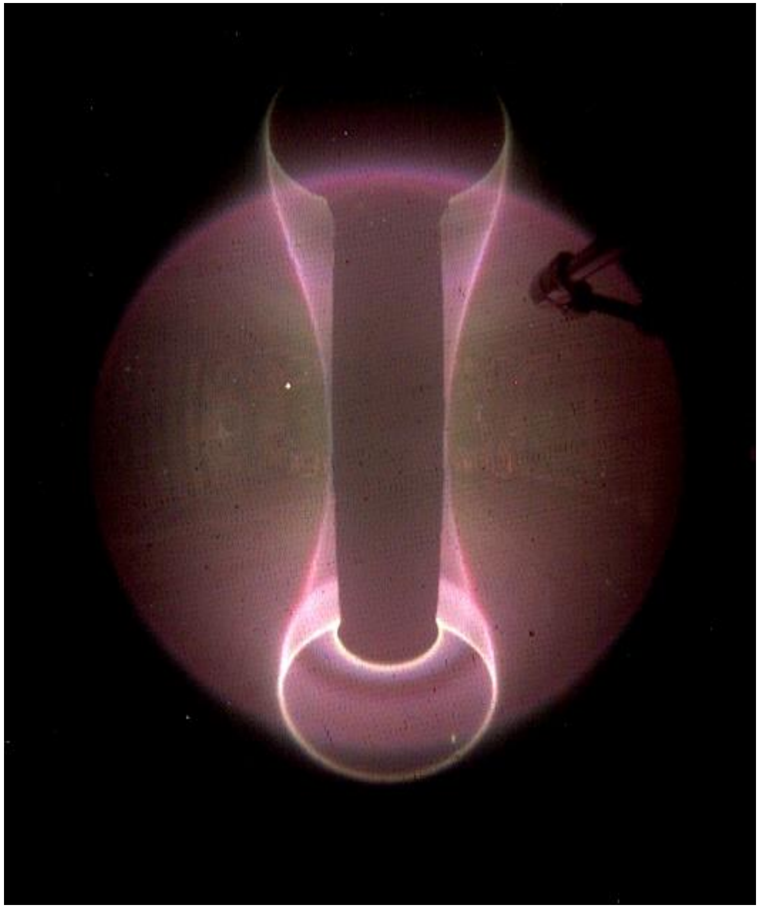

Highlights from first NSTX-U experimental campaign

- Rapid development of high-performance discharges in first 10 weeks of operation
  - Operated at reduced fields: $B_{T0} \leq 0.65T$, $I_p \leq 1MA$
  - Wall conditioning: Helium GDC + boronization
- Stationary L-mode pulse length ~ 4 times longer than NSTX
  - Supported first experiments on error fields, transport, current drive and fast-ion physics
  - **Will be useful for validating global-ES simulations prior to global-EM**
- H-mode discharges comparable to NSTX performance
  - Matched NSTX highest flat-top volume averaged pressure for $I_p < 0.9MA$

1 MW NBI L-modes

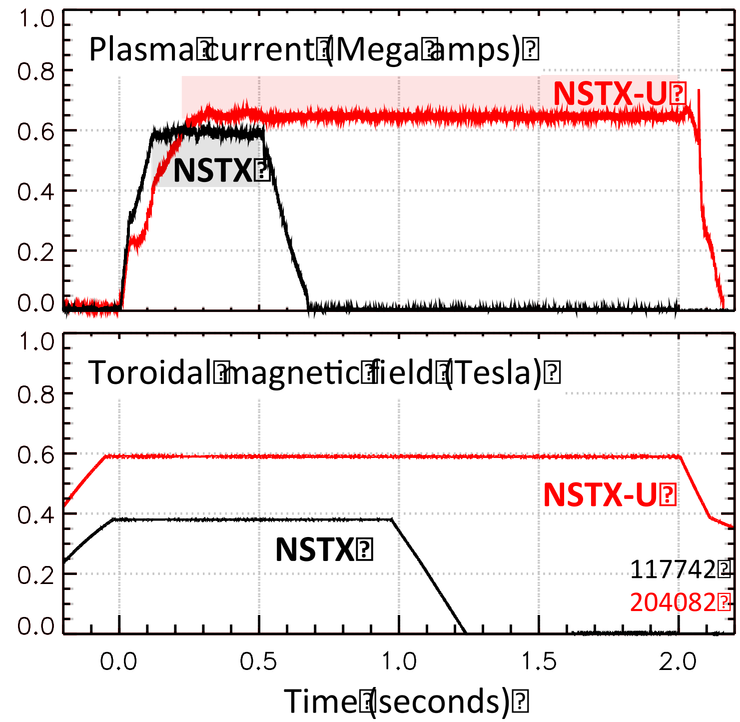

Have already observed changes in GAE stability using 2^{nd} NBI sources

- Injection of 2^{nd} NBI modifies fast-ion phase space, improves stability of fast-ion modes [Fredrickson, APS 2016]
  - Suppression time ~10ms
  - Observations consistent with model of cyclotron-resonant drive of GAE

- Future experiments will probe GAE/CAE activity and correlation with $T_{e,0}$

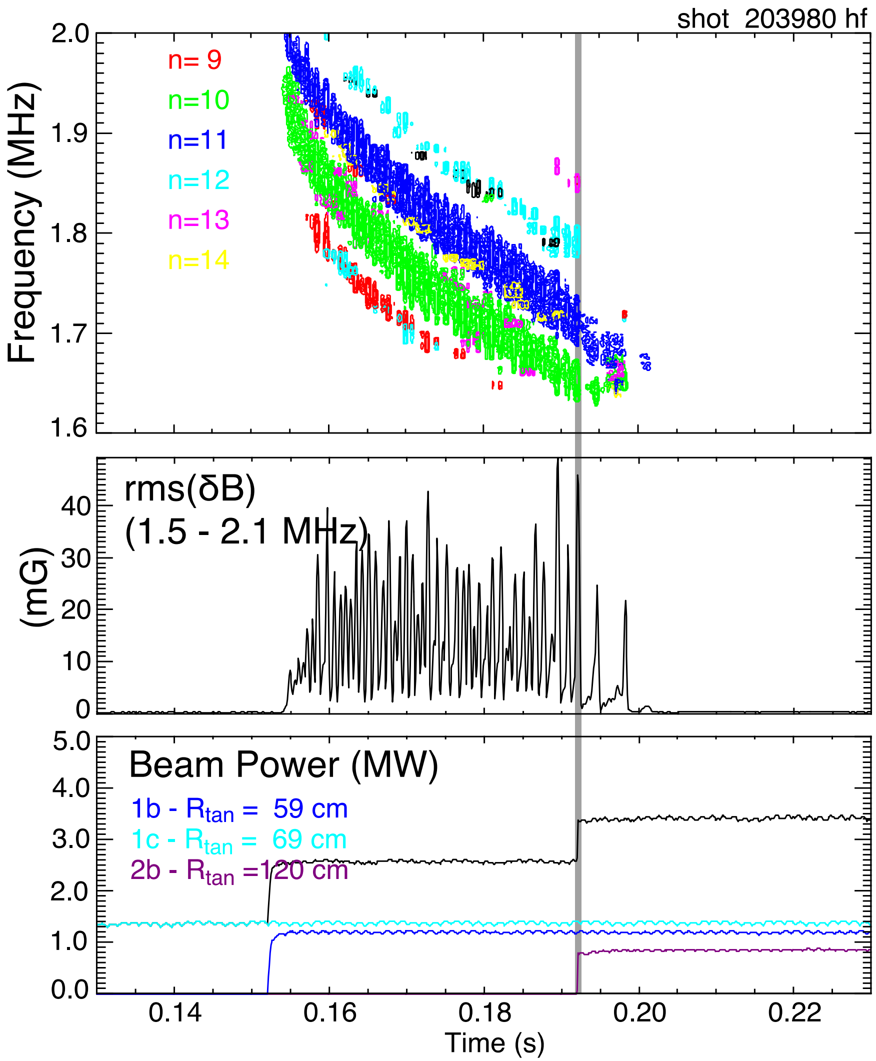

Summary & outlook: ST transport exhibits unique characteristics, challenges theory validation

- Ion thermal transport follows collisional (neoclassical) theory
- Energy confinement scales inversely with collisionality, $\tau_E \sim 1/\nu$

- Numerous drift wave instabilities predicted with different scalings, structure
  - Local theory adds unnecessary complication – **major desire for robust, global electromagnetic simulations (core and edge)**
- Also need to account for fast-ion driven GAE/CAE effects on χ_e

- First NSTX-U operation completed, with significant commissioning of control, heating & diagnostics
- Future transport experiments will take advantage of facility enhancements and improved diagnostic capabilities to validate transport theories and improve predictive capability

THANK YOU!

Linear microtearing instability

- High-m tearing mode around a rational $q(r_0)=m/n$ surface ($k_{||}(r_0)=0$)
  (Classical tearing mode stable for large m, $\Delta'\approx-2m/r<0$)
- In the core, driven by ∇T_e with* time-dependent thermal force $\Rightarrow$ *requires collisionality*

Conceptual linear picture

- Imagine helically resonant ($q=m/n$) δB_r perturbation $\quad \delta B_r \sim \cos(m\theta - n\varphi)$
- δB_r leads to radially perturbed field line, finite island width $\quad w = 4\left(\frac{\delta B_r}{B}\frac{rR}{n\hat{s}}\right)^{1/2}$
- ∇T_e projected onto field line gives parallel gradient $\quad \nabla_{||} T_{e0} = \frac{\vec{B}\cdot\nabla T_{e0}}{B} = \frac{\delta B_r}{B}\nabla T_{e0}$
- Time-dependent parallel thermal force (phase shifted, $\sim i\omega/\nu^* n_e \nabla_{||} T_e$) balanced by inductive electric field $E_{||}=-dA_{||}/dt$ with a δB_r that reinforces the instability

- Instability requires sufficient ∇T_e, β, ν_e (differences predicted in the edge)
- **Not explicitly driven by bad-curvature**

*e.g. Hazeltine et al., Phys. Fluids (1975); Drake & Lee, Phys. Fluids (1977); A. Hassam (1980)

CAE mode-conversion to kinetic Alfvén waves (KAW) predicted to transfer core NBI power to mid-ρ electrons

1) GAE/CAEs cause large χ_e through stochastic orbits (N. Gorelenkov, NF 2010)
2) CAEs also couple to KAW - Poynting flux redistributes fast ion energy near mid-radius, $E_{||}$ resistively dissipates energy to thermal electrons
   - $P_{CAE\rightarrow KAW}$ ~ **0.4 MW** from QL estimate + experimental mode amplitudes
   - $P_{e,NBI}$ ~ **1.7 MW** for ρ <0.3, NBI power deposited on core electrons

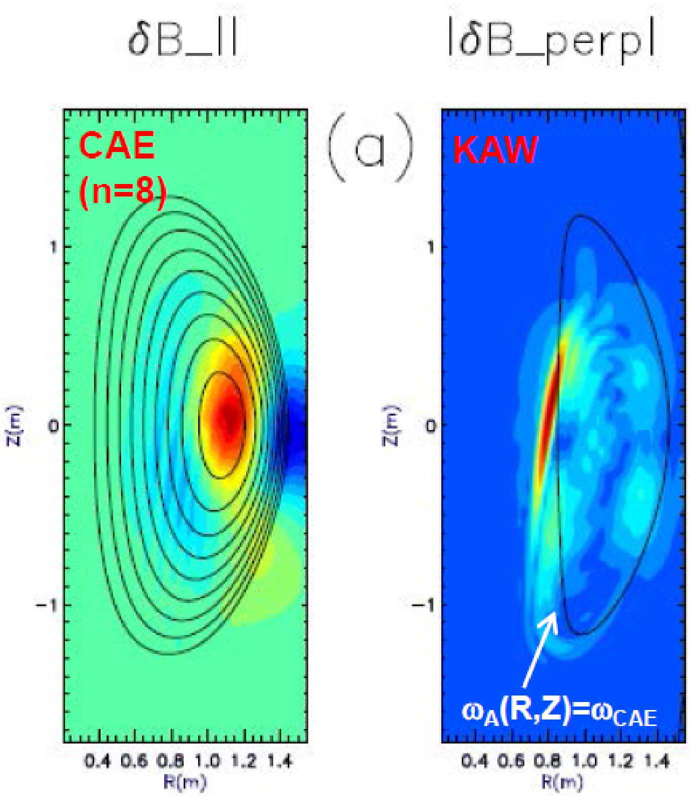

Up to 25% of electron heating power transferred to KAW off-axis

HYM code
E. Belova, PRL 2015

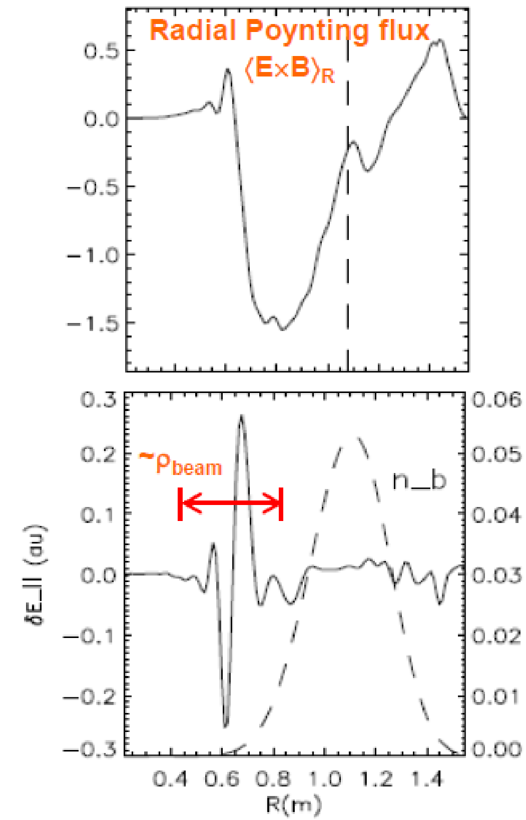

Steady progress in error field correction, plasma control and NBI heating improved H-mode performance

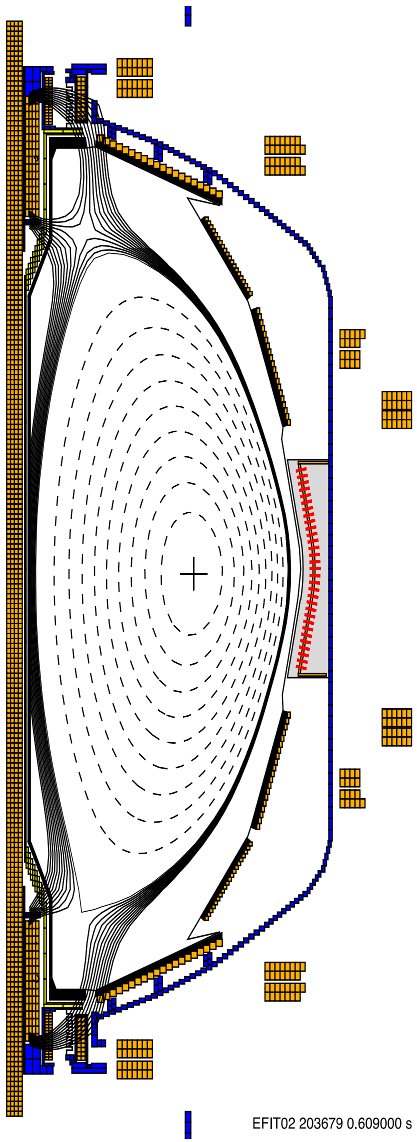

202946 Feb – no EFC
203679 March – EFC v1
202112 April – EFC v2
202118 April – EFC v2

Developments in error field correction (EFC) and shape control enable stable operation at high elongation and I_p.

Density control achieved with regular type-I ELMs.

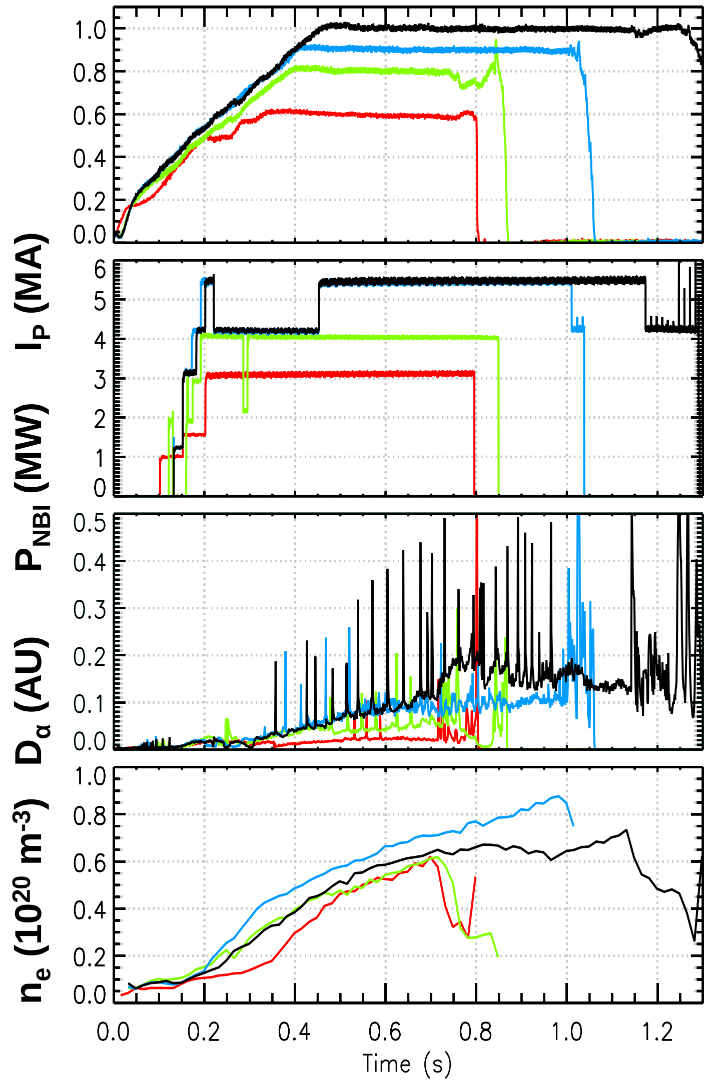

H-mode consistent with NSTX performance operating above no-wall limit with minimal MHD activity

- Achieved target scenario with L-H transition early in discharge
  - Enables highly shaped plasmas with periods of reduced MHD activity operating above no-wall stability limit

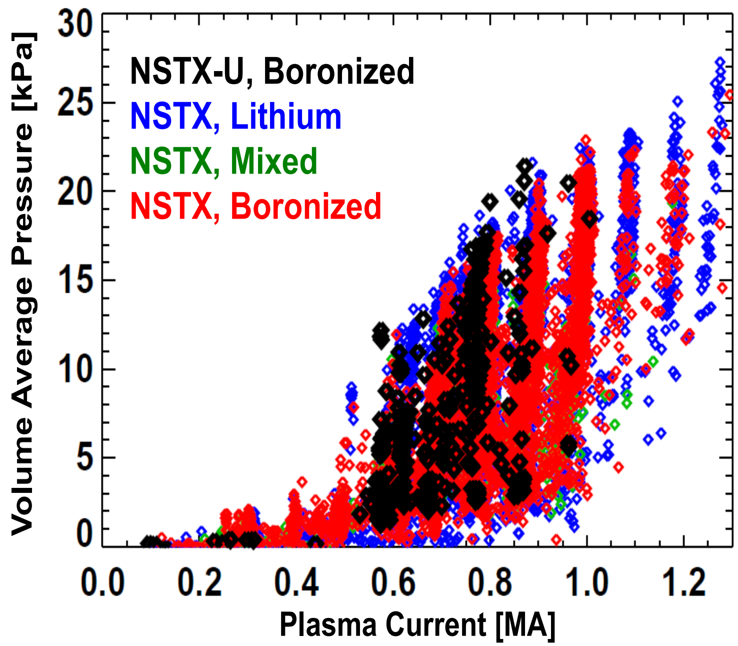

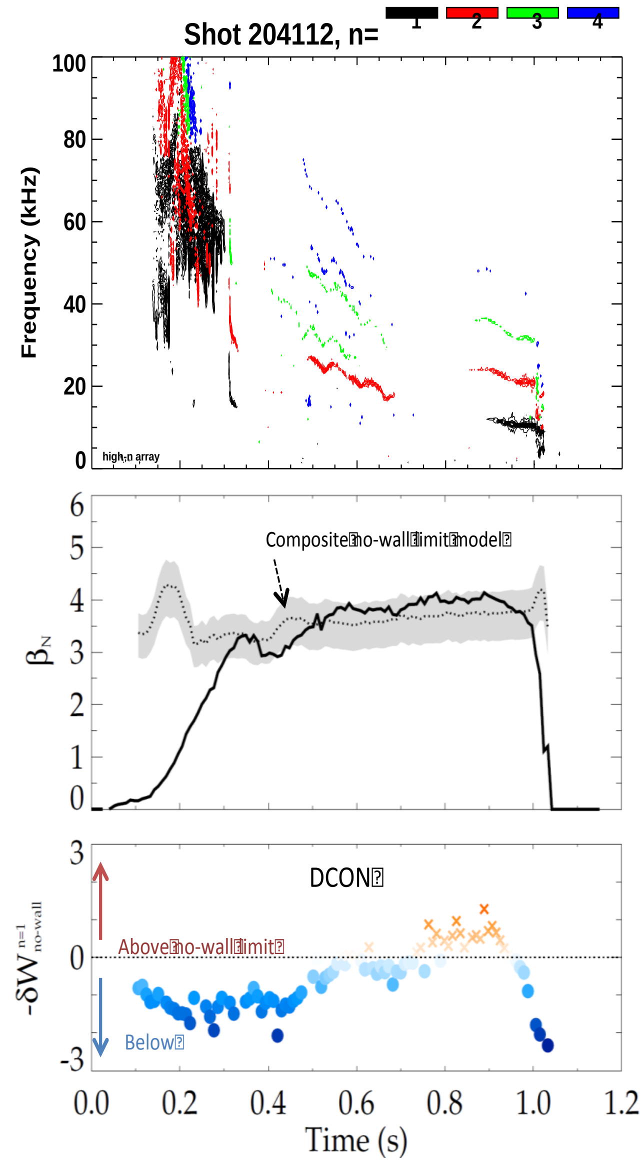

Improvements in the plasma shape control enabled the development of high-performance discharges

- Vertical stability is more challenging at higher aspect ratio (A)
  - Motivated improved detection of vertical plasma motion
  - Achieved NSTX elongation at matched l_i, despite larger aspect ratio

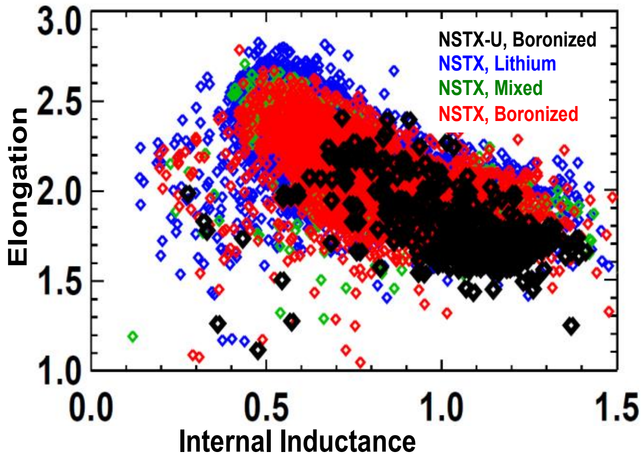

- Larger change in the ohmic fringe field contribution to the equilibrium field
  - Requires active control of the X-point location → not a routine tool on NSTX
  - Multi-threaded rtEFIT enables equilibrium at larger grid resolution and including wall currents

- Diverting and maintaining an inner gap more challenging at higher A
  - Conventional tokamaks have inboard coils, whereas STs do not
  - Actuator sharing algorithm allows the inboard gap to be controlled with adjustments to the X-point and outboard gap requests.